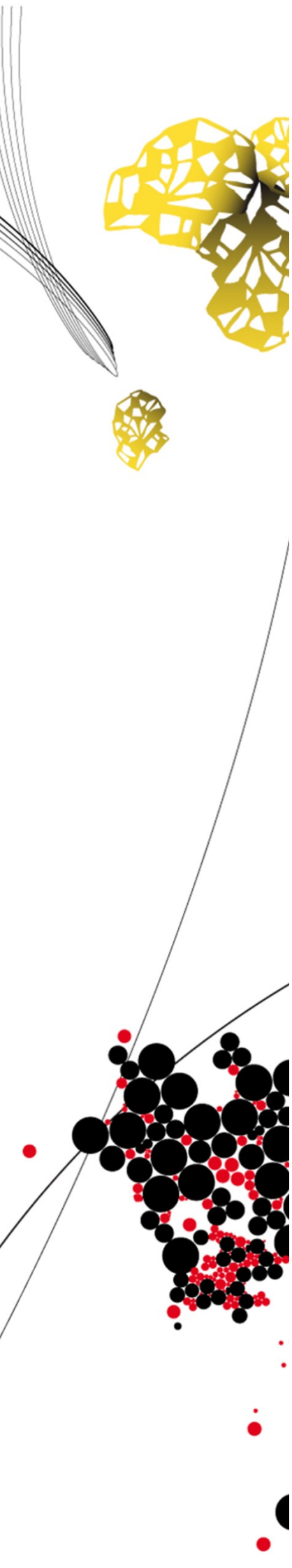

UNIVERSITY OF TWENTE.

Faculty of Electrical Engineering, Mathematics & Computer Science

AM/PM Conversion in Transceiver Systems

S. van Zanten

Bachelor of Science Thesis

June 2017

Daily Supervisor:
A.I. Inácio, M.Sc.
Assignment Committee:
A.I. Inácio, M.Sc.
dr.ir. A.J. Annema
dr.ir. M.J. Bentum

Integrated Circuit Design Group
Faculty of Electrical Engineering,
Mathematics and Computer Science
University of Twente
P.O. Box 217
7500 AE Enschede

Abstract

One nonlinear effect in transceiver systems is the phase modulation at the output due to amplitude modulation at the input (AM/PM conversion). These changes in phase are undesired and limit the performance of RF systems. For the development of new technologies like advanced radar, suppression of AM/PM conversion effects will be vital. This research has focussed on characterizing these effects in a simplified model to gain insight that can be used to synthesize better transceiver systems.

To this end, a first-order low-pass RC-circuit with a nonlinear capacitor has been presented as a simplified equivalent circuit to heterojunction bipolar transistors (HBTs) for the modelling of AM/PM conversion effects in transceiver systems. Two different analyses have been performed to characterize the AM/PM conversion effects in this simplified RC-circuit after which the impact of circuit parameters on the effects has been identified. To deepen insight, several simplifications and assumptions have been introduced in both analyses; their impact on the model accuracy has been considered.

First, a frequency domain analysis has been conducted to characterize the nonlinear phase component of the fundamental frequency that depends on the input amplitude. This model is only valid for modelling weak nonlinearities due to the omission of the influence of higher harmonics, but has shown to be a good approximation to AM/PM conversion in HBTs for relatively small input amplitude values. A second method does include these higher harmonics; this time domain based analysis of the deviation in zero-crossing timings was found to hold for slightly stronger nonlinearities in HBTs.

Theoretical analysis in both the frequency and time domain indicated that the AM/PM conversion effects in the first-order low-pass RC-filter could be reduced by reducing either the value of the resistor, the value of the third-order nonlinear capacitance constant or the input frequency. Simulations have verified these claims, but have also shown that the cut-off frequency plays a major role in the accuracy of the theoretical approximations.

0 Table of Contents

1 Introduction

Front-ends in RF systems handle high-frequency signals; they impose strict requirements on the circuitry of the band-pass filter, low-noise amplifier, local oscillator and mixer that generally comprise such signal chains. Linearity imposes a major limit on the performance of RF circuits and therefore plays a significant role in RF system development. Recent developments in mobile communications technology have strengthened the need for proper modelling of nonlinear effects, as intermodulation effects and crosstalk become increasingly more important in the synthetization of better RF front-ends [1]. Another nonlinear effect is the phase deviation as a result of the unwanted amplitude modulation of the input signal (AM/PM conversion).

The origin of AM/PM conversion effects can be found in active devices like the transistor. Nonlinearities in transistors have been the subject of many research papers which have led to the acquisition of mathematical models, simulations and experimental results [2], [3]. Due to the improved performance of heterojunction bipolar transistors (HBTs) in RF applications over traditional BJTs, research focus has partly shifted to these devices [4].

Recent research on AM/PM conversion effects in HBTs has been directed to effect optimization [5], the development of physical models of both AM/AM and AM/PM effects [6] and experimental verification of simulation results [7]. A mathematical analysis on the influence of circuit and device properties on AM/PM conversion to benefit the design of RF systems is still lacking. The aim of this research will therefore be to understand and characterize AM/PM conversion effects in HBTs by presenting (simplified) mathematic models, verifying these models with simulations and using the results to synthesize better transceiver systems (transceivers are systems that share part of the above-mentioned circuitry for both transmission and reception).

2 Report Structure

The structure of this report entails a clear path to the conclusions drawn on the above-mentioned aim of the research. First, the problem statement is introduced. This section contains several supporting questions that will be answered in this report. After the problem statement, the theory needed to understand the concepts at hand, has been presented. This has been done by including a general mathematical characterization of nonlinear systems and a discussion on the tools needed to evaluate AM/PM conversion effects in such systems. The basic theory is succeeded by an analysis of RF systems in which the emphasis has been laid on the origin of AM/PM conversion effects. Several simplifications will be presented that increase insight in the behaviour of the nonlinearities by reducing some of the complexity required in accurately modelling AM/PM conversion effects. The validity of the assumptions that have been used to construct these simplifications will be assessed.

In addition, the effects of AM/PM conversion on the zero-crossings of HBTs have been characterized with a simplified model. Characterizing AM/PM conversion in the time domain through such an analysis on zero-crossings enables looking into the effects of higher harmonics on the output waveform; the influence of the higher harmonics on the time domain wave form cannot be evaluated conveniently when one analyses the phase of the first harmonic in the frequency domain. This limitation on this specific frequency domain analysis makes it more complicated to use it for the evaluation of systems that cannot be approximated by linear behaviour (e.g. strong nonlinear systems). The ability of the time domain analysis to conveniently capture the influence of higher harmonics makes that it is the preferred method for the analysis on zero-crossings in strong nonlinear systems. Therefore, a time domain model to characterize the translation of AM/PM conversion into zero-crossing shifting will be presented and the interchangeability with the frequency domain through the Fourier transform will be addressed. Simulations have been performed to validate this

mathematical model. Results from both mathematical expressions and simulations yielded several conclusions that will be presented and discussed.

3 Problem Statement

As stated in the introduction, the aim of this research will be to characterize AM/PM conversion effects in HBTs, verify the mathematical model with simulations and use the results to synthesize better transceiver systems.

Rephrasing leads to the main research question:

How can mathematical models and simulations on AM/PM conversion effects be used to synthesize better transceiver systems?

Supporting questions have been formulated to increase insight in the components the answer to the main question is expected to contain, see below.

1. How can AM/PM conversion be mathematically characterized?
2. Noting that a model of a Heterojunction Bipolar Transistor (HBT) will be used to represent the transceiver system, which properties characterize the performance of such a transistor?
3. How can the relation between the properties of HBTs and AM/PM conversion effects be characterized?
4. Noting the answer to question 3, how can AM/PM conversion effects in transceiver systems be mathematically characterized?
5. How can AM/PM conversion effects in HBTs be simulated in a simple enough, yet accurate, model?
6. How can this model be used to verify mathematical models on the relation between AM/PM conversion effects and HBT characteristics?
7. How do the conclusions extracted from the mathematical model and simulations for HBTs extend to transceiver systems in general?

Note that the supporting questions have been numbered, not bulleted, as they represent the structure of the approach to the answer to the main research question. The Theory section in this report will contain the mathematical analysis required to answer the above questions. The Method section will cover the verification of these mathematical results with simulations.

4 Theory

This section contains the theory needed to answer the research question in the Problem statement section.

Before an analysis into the transfer of amplitude modulation at the input into phase modulation at the output can be performed, it is necessary to classify the type of systems in which AM/PM conversion can occur. The analysis that will be required to accurately and correctly characterize AM/PM conversion depends on the type of system it will be applied to. In the case that approximations are applied (that can for instance cover the need for a reduction in complexity), its limitations must be known and they, too, depend on the system the approximation is applied to. The first three sections of this chapter will therefore contain both an explanation on the types of systems that can exhibit AM/PM conversion and the analysis techniques that can be applied to model them.

The remainder of this chapter describes what elements contribute to the manifestation of AM/PM conversion in transceivers and how these elements and their relation to AM/PM conversion can be modelled in a simple, yet accurate enough, model.

4.1 Characterizing systems and their relation to AM/PM conversion

The conversion of Amplitude Modulation at the input of a system into Phase Modulation at the output (AM/PM Conversion) is a nonlinear effect. The reason for this becomes apparent when one looks at the characterization of linear systems. In a generic linear system, if the outputs in response to inputs $x_1(t)$ and $x_2(t)$ are expressed as

$$y_1(t) = f[x_1(t)]$$
$$y_2(t) = f[x_2(t)]$$

then,

$$ay_1(t) + by_2(t) = f[ax_1(t) + bx_2(t)].$$

Since modulation of the input amplitude can never yield a modulation of phase at the output if this output is expressed as the linear combination of responses to individual inputs, only a nonlinear system could potentially generate AM/PM conversion. This means that linear circuit analysis tools cannot be used to exactly model these effects. This does not mean, however, that linear circuit analysis cannot be used at all, as it can be an effective way to simplify complex nonlinear circuits. Next to that, several researchers have looked into extending linear analysis methods to nonlinear versions. An example is the extension of the phasor method to model harmonic distortion in weakly nonlinear circuits [8]. The next section will discuss nonlinear systems and their relation to AM/PM conversion effects.

4.2 Nonlinear systems

As previously mentioned, nonlinear systems are all systems that do not exhibit linear behaviour. They can be divided into two categories: static or dynamic nonlinear systems. An example of a dynamic nonlinear system is a system that contains one or more storage elements. On the other hand, 'memoryless' or 'static' systems generate outputs that do not depend on past values of the inputs.

A general mathematical description of such a static system can be given by

$$y(t) = \alpha_0 + \alpha_1 x(t) + \alpha_2 x^2(t) + \alpha_3 x^3(t) + \cdots$$

Note that in the case of weakly nonlinear circuits, this expression is truncated to a certain order, meaning that such a system can be properly approximated by the terms up to that order. For transistor distortion (that is often small [2]), the expressions in this Thesis will be assumed to correctly model the effects when the terms up to and including the third-order are included. Hence, the expression will be truncated after the third-order degree. If this expression would be excited by a carrier wave with a certain amplitude as described by $x(t) = A\cos(\omega t)$, the output of a weakly nonlinear system truncated after the third-order term would be equal to

$$y(t) \approx \alpha_0 + \frac{\alpha_2 A^2}{2} + \left(\alpha_1 A + \frac{3\alpha_3 A^3}{4}\right) cos(\omega t) + \frac{\alpha_2 A^2}{2} cos(2\omega t) + \frac{\alpha_3 A^3}{4} cos(3\omega t)$$

Several conclusions can be extracted from the above expression:

- Memoryless nonlinear systems do not exhibit AM/PM conversion, since the harmonics do not contain a phase-term that could possibly depend on the amplitude of the input.
- Effects of the third harmonic map onto the carrier wave frequency.
- The second harmonic yields a term at DC.

In addition, note that odd-symmetric circuits, like fully differential circuits, have a special property that directly impacts the above result; even harmonics are cancelled out by the odd-symmetric nature of the circuit.

All other nonlinear systems are called 'dynamic' and are capable of storing information which can impact the behaviour of the system. A general mathematical description of a dynamic nonlinear system is given by

$$y(t) \approx \alpha_0 + \alpha_1 x(t-\tau_1) + \alpha_2 x^2(t-\tau_2) + \alpha_3 x^3(t-\tau_3) + \cdots$$

Again, if this system is excited by the same sinusoid and assumed to be weakly nonlinear, one finds

$$y(t) \approx \alpha_0 + \frac{\alpha_2 A^2}{2} + \alpha_1 A\cos\big(\omega(t-\tau_1)\big) + \frac{3\alpha_3 A^3}{4}\cos\big(\omega(t-\tau_3)\big) + \frac{\alpha_2 A^2}{2}\cos\big(2\omega(t-\tau_2)\big) + \frac{\alpha_3 A^3}{4}\cos\big(3\omega(t-\tau_3)\big)$$

As was the case with static nonlinear systems, the following holds for dynamic nonlinear systems:

- Effects of the third harmonic map onto the carrier wave frequency.
- The second harmonic yields a term at DC.

However, in contrast to static systems, one finds that the system's timing constants τ_1, τ_2 and τ_3 determine the phase of the output. These timing constants depend on the configuration of the system and can therefore also depend on the input amplitude. In other words, it is possible that AM/PM conversion effects manifest themselves in dynamic nonlinear circuits.

4.3 Analysing dynamic nonlinear systems

Since only dynamic nonlinear circuits can exhibit AM/PM conversion, it is necessary to use analytical methods that can cover such systems. It was already mentioned in the introduction that linear circuit analysis methods can be used as a basis to approximate nonlinear systems if their nonlinearities are small. The main advantage of using this method is the reduction in complexity that can be achieved (linear circuit analysis methods are often simpler than nonlinear versions due to for instance the possibility to use the technique of superposition or to use phasor analysis). The main disadvantage is the reduction in accuracy of the results that linearizing nonlinear effects leads to.

To increase this accuracy, methods can be used that specifically consider the dynamic nonlinear nature of circuits, but a disadvantage in general for such methods is that they can be much more complicated and require more computations to obtain results. One method to calculate the steady-state response of dynamic nonlinear systems is called 'harmonic balance'; it uses Kirchhoff's Current Law written in the frequency domain.

An alternative to the 'harmonic balance' method is the 'Volterra series' approach. This method is also based on a recursive set of steps that compute the response of the circuit without the need to solve nonlinear equations. As did the 'harmonic balance' method, the 'Volterra series' method has some disadvantages [2].

First, if the rate of convergence of a circuit is not rapid, the cumbersome higher-degree terms cannot be neglected (usually the system is then in a strong nonlinear regime). As a result, this method cannot conveniently represent gross nonlinearities, as computer programs will be required to perform the mathematical analysis (often limiting insight). Second, the results of this multidimensional transform cannot be easily transformed to the time domain and finally, the technique is not useful for determining the stability of a nonlinear differential equation.

When it comes to modelling transistor distortion however, the use of the 'Volterra series' offers distinct advantages. The method can be used to represent frequency dependent systems, such as amplifiers containing transistors. In addition, the nonlinearities that are of interest to the modelling of AM/PM conversion effects exhibit small changes such that the lower-degree terms are sufficient for an accurate model: the transistors are assumed to be working in the weakly nonlinear region. The main advantage of using this method is that the Volterra kernels contain the phase modulation of the system with respect to certain signals at the input. Hence, the 'Volterra series' method is capable of modelling AM/PM conversion effects. Many literature sources have covered the use of the Volterra series, see for instance [9, p. 81].

The complex nature of nonlinear effects in general, and therefore also of AM/PM conversion, requires deeper understanding than is often needed for the analysis of linear effects. Therefore, to increase the understanding of AM/PM conversion, simplifications will be made that increase insight. This is the main reason why the analysis in the following sections will be based on linear circuit analysis methods in which nonlinear expressions will be substituted. If needed and beneficiary for the results of this Thesis, the accuracy of the results can be increased by performing a Volterra series analysis.

4.4 The origin of nonlinear effects in transceiver systems

To be able to model the AM/PM conversion effects in transceiver systems, one must first know why they occur and by which nonlinearities they are caused. Therefore, nonlinearities in transceivers will now be looked into. A general representation of a transceiver can be found in Figure 1.

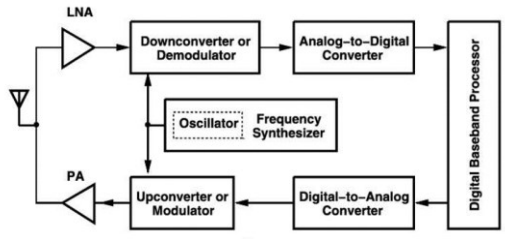

Figure 1: Schematic representation of a transceiver [9].

Every block of the transceiver in Figure 1 contains nonlinear elements. However, most of these nonlinear elements can be properly approximated by linear behaviour. The active nature of the circuitry comprising transceivers is directly related to nonlinearities that cannot be completely linearized. Due to the amplifying properties of certain transistor configurations, these nonlinear effects tend to become dominant. This is why the focus of this research will be set to the transistor, or more specifically, to the heterojunction bipolar transistor as these devices are used in higher-frequency and/or higher power RF-circuits.

4.5 Modelling nonlinearities in HBTs

Maas et al. [4] have published a model for the heterojunction bipolar transistor. They use the method of nonlinear currents based on the Volterra series to model nonlinear effects that are present in systems containing HBTs, due to intermodulation. The linearized and simplified equivalent circuit (without parasitics) of the HBT has been depicted in Figure 2.

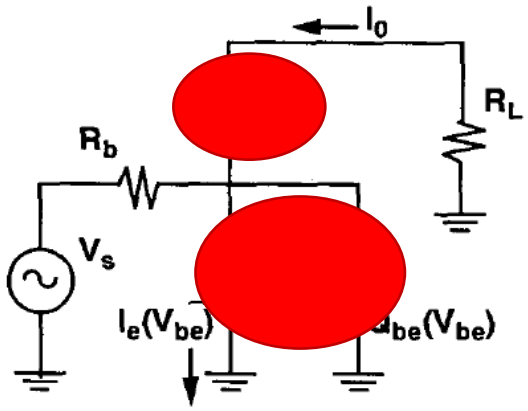

Figure 2: Simplified, linearized equivalent circuit of the HBT [4]. The main nonlinearities have been indicated with a red circle.

In addition, the authors [4] present a complete nonlinear equivalent circuit of the HBT including parasitics, this can be found in Figure 3. This model differs from the one in Figure 2 as also relatively small properties contributing to the device's nonlinearity have now been modelled with circuit elements.

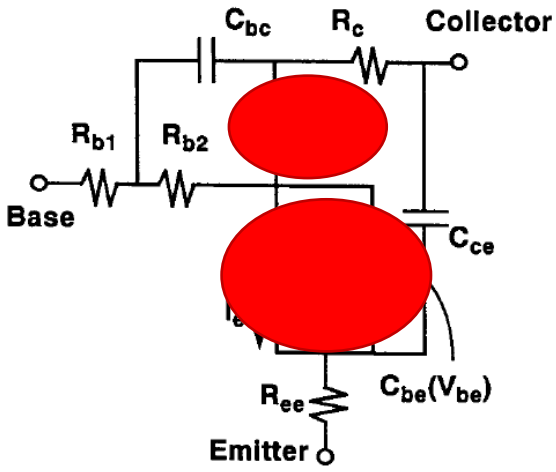

Figure 3: Complete nonlinear equivalent circuit of the HBT [4]. The main nonlinearities have been indicated with a red circle.

The main nonlinearities in HBTs are the depletion region, modelled as an ideal junction diode, the capacitive junction and the nonlinear current source $I_C(I_E)$ [4, p. 446], see the red circles in Figures 2 and 3.

Although the model has been used in the paper to model intermodulation distortion in HBTs, it can be applied to aid the modelling of the AM/PM conversion effects as these are caused by the same nonlinearities. However, before the relation between AM/PM conversion and the above presented nonlinearities can be analysed, it is important to verify the model; an incomplete or incorrect model might fail to properly identify the nonlinearities that cause AM/PM conversion and/or fail to enable the derivation of the mathematics needed to evaluate the influence of HBT nonlinearities on AM/PM conversion. To this end, an analysis aimed at verifying the scientific basis of the model has been applied to 'Intermodulation Distortion in Heterojunction Bipolar Transistors' [4], please refer to Appendix 10.1.

The conclusion of this analysis is that the model has been sufficiently justified with a verification of model predictions through measurement results. However, the information that is necessary to

reproduce the findings is not complete, this makes verification by others difficult. Considering that the measurement results mainly cover intermodulation distortion and not AM/PM conversion, the verification of these results is of little importance to this thesis. In addition, in the case that the model is incomplete, the nonlinearities that the model is then missing are small as the main nonlinearities have already been modelled (depletion region and nonlinear current source). These two arguments will be considered to sufficiently justify the use of this model to model AM/PM conversion effects in HBTs.

Consider the model in Figure 3 again; it contains nine components that together model the behaviour of an HBT. To be able to better understand how AM/PM conversion works, several assumptions will be made that considerably simplify the circuit:

1. The parasitic capacitances C_{bc} and C_{ce} are assumed to be neglectable.
2. The parasitic resistors R_{b1}, R_{b2} and R_{ee} are assumed to be neglectable.
3. Capacitance C_{be} will be modelled to contain both the nonlinear effects of its own capacitance and the nonlinear effects of the diode placed in parallel.

The nonlinear current source of the HBT is one of the dominant nonlinearities. This poses a problem to the mathematical evaluation of the HBT's behaviour as it means that the nonlinearity of the base-emitter junction will be amplified by a nonlinear function. As a result, evaluating the nonlinearities individually will be difficult. Therefore, to simplify the analysis into AM/PM conversion, the nonlinearity of the base-emitter junction will be looked into separately by assuming that the amplification is sufficiently linear and that the influence of the collector current on the signal at the base is neglectable.

Note that in the above proposed case where the amplification of the voltage across the base and emitter can be considered sufficiently linear, the current source included in the model is not needed for the characterization of the AM/PM conversion effects as it would only linearly amplify the signal. Extending this reasoning, one can state that if resistor R_c is linear, the voltage drop across it will be directly (and linearly) proportional to the voltage across the base-emitter through $V_c \approx I_c R_c \approx \alpha V_{be} R_c$. Considering that the small signal output of the transistor is then also linearly related to the voltage drop across R_c, **the relation between input amplitude modulation and output phase modulation will be reduced to the relation between input AM and the phase modulation at the base of the HBT**. This relation will therefore be the main focus of this research.

Although the dominant nonlinearities will be part of the simplification, question remains if the omission of 7 of the 9 components and the merger of the diode and capacitor into one nonlinear capacitance simplifies the circuit too much. The discussion section will contain an analysis on the impact of these simplifications on the results.

After taking into account all assumptions mentioned above, the source impedance and base-emitter capacitance will form a first-order low-pass RC-circuit of which the nonlinear capacitor is the main source of nonlinearities. Hence, the next section will cover its effects on AM/PM conversion.

4.6 AM/PM conversion in a nonlinear capacitor

A nonlinear capacitor is both a dynamic and a nonlinear system, therefore it can cause AM/PM conversion. To see how, consider the following capacitor expressions that apply to Figure 4:

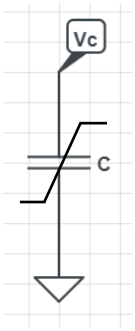

Figure 4: Nonlinear capacitor.

$$C_L = C_1$$
$$C_{NL2} = C_1 + C_2 \cdot V_c$$
$$C_{NL3} = C_1 + C_2 \cdot V_c + C_3 \cdot V_c^2$$

where C_1 is the linear capacitance constant, in Farad
C_2 is the second-order capacitance constant, in Farad
C_3 is the third-order capacitance constant, in Farad
V_c is the voltage across the capacitor, in Volts.

Figure 5 contains a plot of the capacitance curves described above.

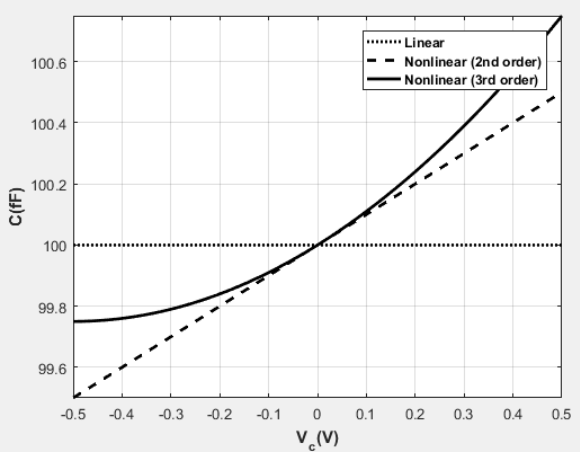

Figure 5: Plot of the capacitance expressions over V_c. C_1, C_2 and C_3 have been set to 100 pF, 1 pF and 1 pF respectively.

If one would apply two different sinusoidal waves across the capacitor, as depicted in Figure 6, the nonlinear capacitance values will change over time, see Figure 7.

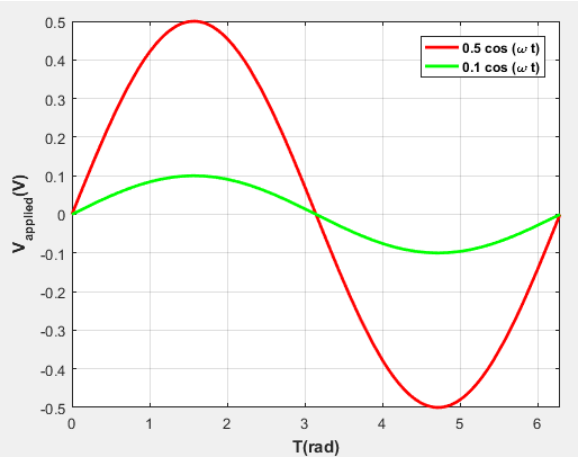

Figure 6: Plot of the relation between voltage and time of two sinusoids with different amplitudes.

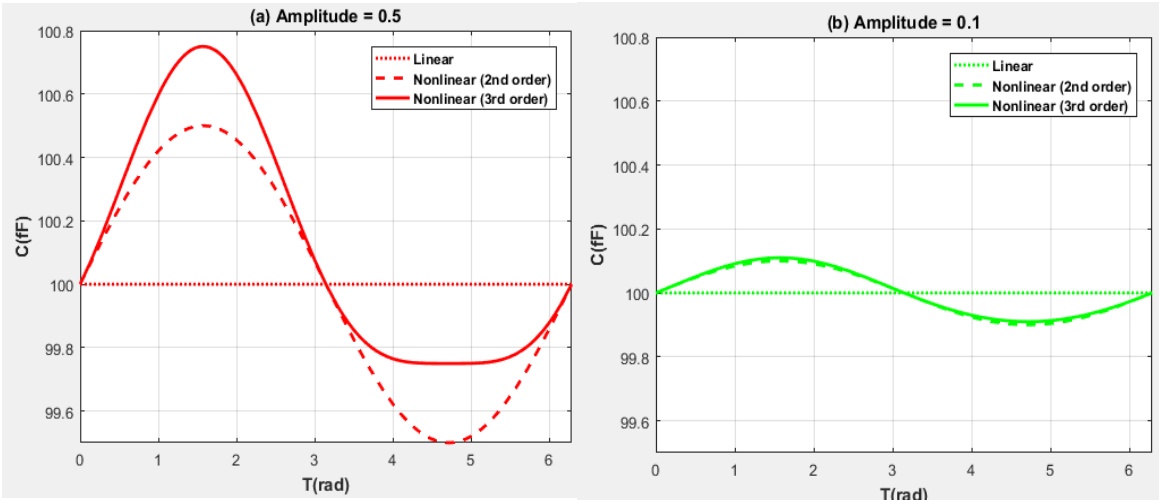

Figure 7: Plots showing the capacitance variation over time for the capacitance values C_L, C_{NL2} and C_{NL3} for the two voltage functions defined in Figure 6.

Figure 7 shows that the linear capacitance expression has no dependence on amplitude, see the dotted line in both plots. However, the nonlinear expressions (represented by the solid and dashed lines) do depend on the amplitude of the signal applied across them. For both the 2nd-order and 3rd-order dependence, the Root Mean Square (RMS, or quadratic mean) value is different and amplitude dependent. This can be seen in Figure 7 by comparing the RMS value of the dashed and solid lines in both plots for 2nd- and 3rd-order respectively.

Applying an amplitude-modulated signal across a nonlinear capacitor would generate a directly related variation of the capacitance. The capacitance value determines the behaviour of the system and has an impact on the way the system transfers the input signal to the output: in this case, the transfer function will change with a change in input amplitude due to its dependence on the nonlinear capacitor. This effect is the foundation of the manifestation of AM/PM conversion effects in circuits containing nonlinear capacitors or similar components that manifest nonlinear dynamic behaviour. Note that in the case of a regular sinusoid at the input without any modulation in amplitude, no AM/PM conversion will take place, as there would be no change in quadratic mean of the capacitance.

The above presented theory shows that the capacitance constants can exert influence on AM/PM conversion effects in transceiver systems. Now that it is clear that the nonlinear capacitances in transistors are a cause for AM/PM conversion, one can take a step back and consider how these conclusions apply to the simplified model of the HBT: the first-order low-pass RC-circuit. This information can subsequently be used to present solutions that can be applied to improve this unwanted behaviour.

4.7 AM/PM conversion in a first-order low-pass RC-section

Consider the first-order low-pass RC-circuit depicted below as an equivalent circuit to the HBT, in Figure 8.

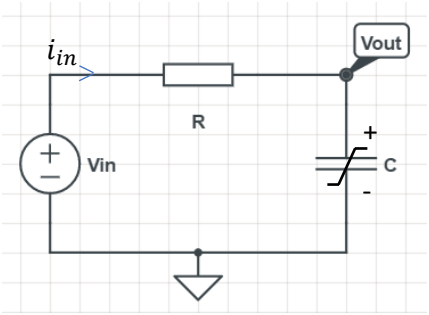

Figure 8: First-order low-pass RC-filter.

The capacitor is weakly nonlinear and its capacitance will be described by the same terms as in Section 4.6:

$$C(V_C) = C_1 + C_2 \cdot V_c + C_3 \cdot V_c^2 = C_1 + C_2 \cdot V_{out} + C_3 \cdot V_{out}^2$$

in which V_c is the voltage across the capacitor which is equal to V_{out}, in this particular case.

To calculate the phase of the output at the fundamental frequency, this capacitance value can be inserted in the differential equation of this circuit:

$$R(C_1 + C_2 \cdot V_{out} + C_3 \cdot V_{out}^2) \cdot \frac{dV_{out}}{dt} + V_{out} = V_{in}$$

in which V_{out} is the output voltage of the circuit and V_{in} is the voltage applied at the input.

The solution of this equation can be approximated through applying the Volterra series, discussed in the Section 4.3.

However, the elaborative nature of the higher order kernels makes it hard to evaluate the nonlinear output of the circuit by hand. Next to that, extracting information on the phase from Volterra series is complex. Therefore, to increase insight in circuit behaviour, linear circuit analysis tools will be applied as proposed in Section 4.3. Approximation the circuit behaviour through linear circuit analysis will be considered justified due to the small nonlinear capacitance constants C_2 and C_3 in relation to the linear coefficient C_1 (thus assuming a weakly nonlinear regime). The validity of this assumption will be covered in the discussion section of this report. Appendix 10.2 contains the mathematics required to obtain the following approximation of the amplitude dependent phase, related to Figure 8:

$$\phi(A) = -\frac{RC_3\omega_{in}A^2}{2}$$

in which
R is the value of the resistor, in Ohms
C_3 is the value of the third-order capacitance constant, in Farad
ω_{in} is the value of the frequency applied to the input, in rad/s
A is the peak-amplitude of the input signal, in V.

Note that next to the above-mentioned assumption that the capacitance can be approximated with linear circuit analysis methods by considering the average of its capacitance value with a periodic variation (assuming the periodic variation of the envelope of the input signal) over time, two other assumptions have been made:

- The input frequency is assumed to be well below the cut-off frequency of the circuit ($RC\omega \ll 1$).

- The system is fully differential, meaning that the even harmonics are suppressed.

The approximated relation between input amplitude and the phase shift shows that there are several parameters that exert influence on the magnitude of this phase shift:

- The time constant of the third-order nonlinearity within the RC-circuit (RC_3).
- The fundamental frequency of the input (ω_{in}).
- The peak/rms amplitude of the input signal (A).

The first two can be altered to minimize the effects of the third parameter, the actual dependence of the phase on input amplitude. According to the approximation, decreasing the time constant of the third-order nonlinearity in the RC-circuit under a fixed input frequency whilst conserving proper biasing of the HBT would decrease the magnitude of AM/PM conversion effects.

However, the bias mode used and also the level at which the HBT is biased determine the magnitude and DC voltage that will appear across the base-emitter capacitance. This has an impact on the nonlinearity that the capacitor exhibits within the circuit and hence reduces the analogy between the low-pass filter and the small signal equivalent of the HBT. Linear approximations cannot be used to model strong nonlinear behaviour and one would expect that with an increase in the strength of the nonlinear behaviour, the accuracy of the approximation will reduce.

The simple first-order low-pass RC-filter should be adjusted to analyse if adjustments can be made such that a better approximation of the behaviour of the HBT can be obtained (that is capable of modelling stronger nonlinearities). Appendix 10.3 contains the mathematical analysis similar to the one in Appendix 10.2, with two additional circuit configurations: Figure 9 includes the internal base resistance and Figure 10 includes the diode in Figure 3, as a linear resistor (the nonlinearities of the diode are still included in the nonlinear expression for the capacitance of the base-emitter junction).

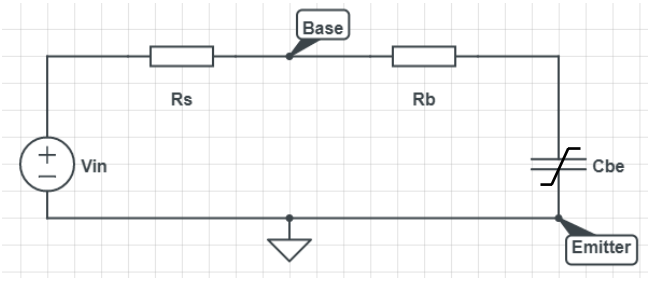

Figure 9: RRC-circuit resembling the simplified internal base-emitter structure of an HBT including the source resistance of the signal applied to the base.

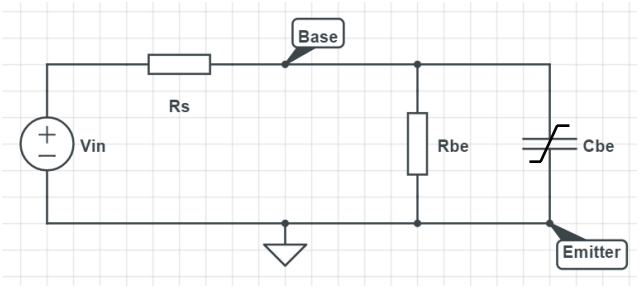

Figure 10: First-order low-pass RC-filter with additional resistor in parallel to the capacitor.

4.8 Zero-crossings in relation to AM/PM conversion

So far, models based on frequency analysis were mentioned. However, time domain can also be used to describe dynamic nonlinear system and therefore also the RC-circuit treated thus far. The theory

discussed before increased understanding of the phenomenon that amplitude modulation at the input of RF-circuits can transfer into phase modulation at the output of such circuits (refer to plots 5, 6 and 7 in section 4.6).

Although the approximations indicate that the magnitude of the effects can be decreased by minimalizing the third-order timing constant of RC-circuit configurations within transistor circuits and by reducing the input frequency, they can never be fully suppressed without losing proper circuit performance. Suppression of AM/PM conversion effects effectively boils down to a trade-off between signal amplitude and suppressing the influence of nonlinearities that cause AM/PM conversion. Maintaining proper circuit operation is paramount to the development of better transceivers and therefore the reduction of AM/PM conversion effects is limited and an analysis of larger signal swings is required.

As the input amplitude of the signal applied to the base of the transistor is increased, the nonlinearity of the device will increase. An increase in amplitude will lead to violation of the bias point as the signal swing is too large to approximate the $V_{BE} - I_c$ curve with a linear approximation. Therefore, increasing the input amplitude too much will push the transistor out of the weakly nonlinear regime and as a result, the frequency domain analysis that has been used up to now is not suitable anymore to analyse AM/PM conversion. Characterizing the phase shift in terms of zero-crossings allows inclusion of higher harmonics on the output signal as the signal is evaluated at certain time instants (thus allowing analysis of all frequencies that comprise the signal at that time instant). This relation between zero-crossings (time-domain) and AM/PM conversion is expected to hold for stronger nonlinear behaviour. The next sections will cover this relation.

4.8.1 Relation between phase and zero-crossing values

In general, the relation between the phase and zero-crossings of any cosine can be characterized by the following. Consider a general representation of a cosine:

$$V(t) = A\cos(\omega t + \phi)$$

The zero-crossings can be found by equating this signal to zero:

$$\begin{aligned} V(t) = 0 &\rightarrow \cos(\omega t + \phi) = 0 \\ \omega t + \phi &= \frac{\pi}{2} + \pi \cdot k \\ t(k) &= \frac{1}{\omega}\left(\frac{\pi}{2} + \pi \cdot k - \phi\right) \end{aligned}$$

The value of the k-th zero-crossing depends on the phase of the signal itself, but how does it depend on the system? The relation between frequency domain descriptions of systems and the phase in the time domain can be characterized as follows. Take a system in the frequency domain:

$$Y(\omega) = H(\omega)X(\omega)$$

Now transform this into a time domain expression [10]:

$$y(t) = |H(\omega)X(\omega)|\cos(\omega t + \arg(H(\omega)X(\omega))) = |H(\omega)X(\omega)|\cos(\omega t + \phi + \arg(H(\omega))$$

One can see that the argument of the transfer function directly translates into a contribution to the phase of the output; this effect will be very important in the following derivation of the relation between AM/PM conversion and zero-crossings. Before proceeding, one should note in addition that, depending on the expression of $X(\omega)$ or $H(\omega)$, $|H(\omega)X(\omega)|$ can also have an impact on the phase of the output.

4.8.2 Approximating the relation between zero-crossings and AM/PM conversion

Based on the same assumptions that were deemed to justify the use of linear circuit analysis tools to model AM/PM conversion effects, the relation between zero-crossings and AM/PM conversion will be mathematically characterized. For this, please consider the first-order low-pass RC-filter in Figure 8 along with its assumptions explained in Section 4.7 once more. An amplitude modulated signal will be applied to it that adheres to the following equation:

$$V_{in}(t) = A\cos(\omega t) = A_c(1 + m\cos(\omega_m t))\cos(\omega t)$$

Appendix 10.4.1 contains the derivation of the following expression:

$$t_{ZC}(k) = \frac{1}{\omega_{in}}\Big(\frac{\pi}{2} + \pi \cdot k + \arctan\Big(\omega_{in}R\Big(C_1 + C_2A_c(1 + m\cos\omega_m t)\cos\omega_{in}t + C_3\big(A_c(1 + m\cos\omega_m t)\big)^2\cos^2\omega_{in}t\Big)\Big)\Big)$$

in which
- t_{ZC} is the value of the kth zero-crossing in seconds
- ω_{in} is the value of the carrier frequency in rad/s
- R is the value of the resistor in Ohm
- C_1, C_2 and C_3 are the 1st-, 2nd- and 3rd-order capacitance constants in F
- m is the modulation factor
- A_c is the peak-amplitude of the carrier wave in Volts
- ω_m is the frequency of the modulator signal in rad/s.

This expression for the zero-crossings can be related to the frequency domain approximation that has been derived and presented in Section 4.7. Considering the limitation of the method that was used to obtain that approximation, the expression obtained through the time domain method can be transferred into a similar approximation as the one in Section 4.7 by considering only the fundamental frequency of the carrier. If one achieves this by filtering out all other frequencies, one can rewrite the above expression for $t_{ZC}(k)$ to the following (note that the amplitude modulation used in this section has been left out to show the analogy):

$$t_{ZC_{(f)}}(k) = \frac{1}{\omega_{in}}\left(\frac{\pi}{2} + \pi \cdot k + \omega_{in}RC_1 + \frac{RC_3\omega_{in}A^2}{2}\right)$$

To increase the accuracy of the model that will be used to analyse the effects of AM/PM conversion, the influence of higher harmonics will now also be included. Hence, the expression for $t_{ZC}(k)$ will be solved for t. Note that the expression still contains the time itself which makes evaluating it difficult. To this end, numerical solvers in Mathematica will be used for the evaluation.

The result has been visualized using Mathematica as well. Consider Figure 11 a-d below, refer to Appendix 10.4.2 for the code. For visualisation purposes, the frequency of the modulation will only be 10 times smaller than the carrier for these plots, it will be a 1000 times smaller in the actual simulations.

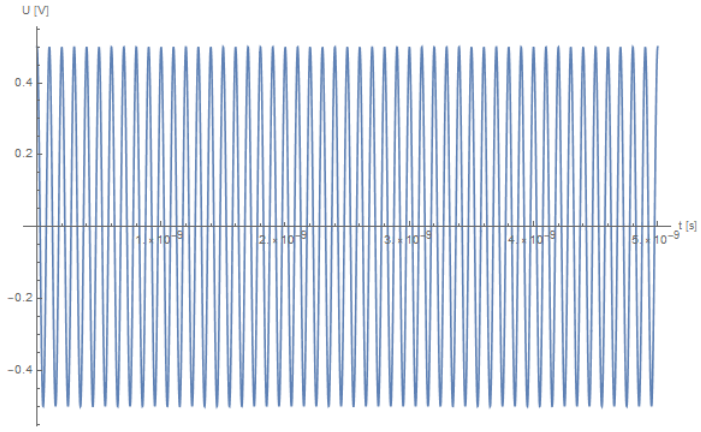

Figure 11a: Carrier wave.

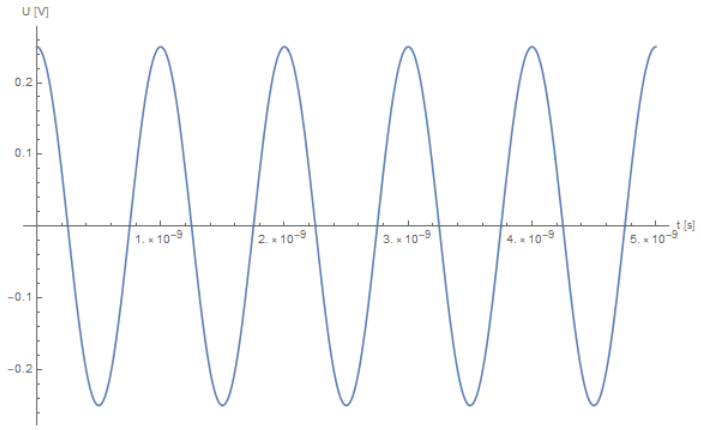

Figure 11b: Signal that will be applied as envelope modulation.

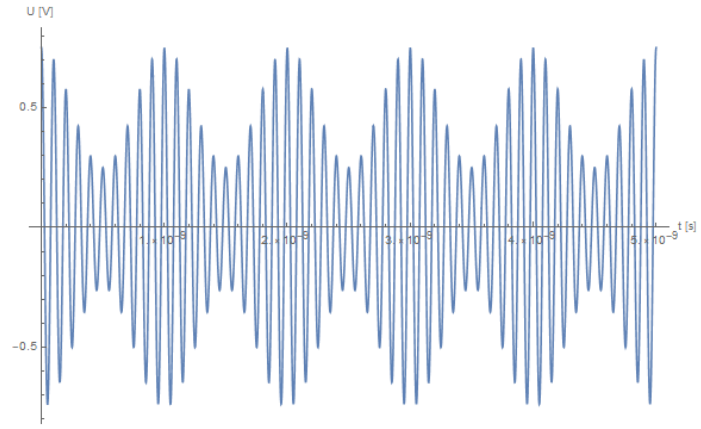

Figure 11c: Amplitude modulated signal.

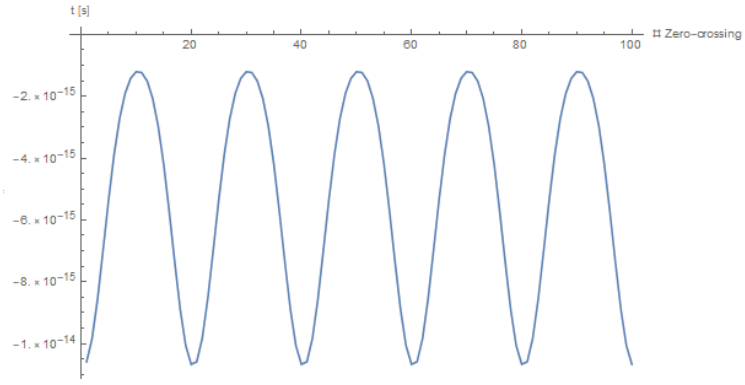

Figure 11d: Conversion of AM to changes in timing of the zero-crossings with respect to the linear circuit (with constant phase).

Figure 11d visualizes the relation between zero-crossings and the modulated phase due to amplitude modulation at the input. Note that the phase of the output can be split into two terms: the insertion phase (or phase of the linear circuit) and the nonlinear phase. The plot of Figure 11d contains only the nonlinear component; the insertion phase has been subtracted such that the direct relation between AM and PM can be evaluated. It is clear that the sinusoidal behaviour of the input amplitude is being converted to sinusoidal deviations in the zero-crossings at the output. The results presented in Figure 11d will be compared to simulations to verify if they properly resemble the behaviour of first-order low-pass RC-filters with a nonlinear capacitor.

4.9 Summary of the theoretical analysis

Conversion of amplitude modulation at the input of a system into phase modulation at the output (AM/PM conversion) has been covered. The effects have been determined to originate from dynamic nonlinear systems within RF circuitry of which the most basic element is the nonlinear capacitor. The fundamental processes that cause AM/PM conversion have been characterized in their relation to several circuits. The first-order low-pass RC-filter section is the most important of these circuits as it has been assumed to be a proper representation of the base-emitter structure of the heterojunction bipolar transistors that comprise RF circuitry.

AM/PM conversion effects in first-order low-pass RC-filter circuits have been characterized through both time and frequency domain representations. Characterization has been done through a linear approximation of nonlinear behaviour; the assumptions used to this end have been explicitly stated and are primarily considered justified due to the weakly nonlinear nature of the transistor mode used.

If the validity of these assumption can be verified through simulations to be conducted (see the Method section), the main benefit of this simplification will be the relative simplicity with which the complex nonlinear AM/PM conversion mechanisms in HBTs can be understood. Next to that, the simulations will aim to verify the accuracy of the frequency based analysis and the question whether it will be suited to analyse the effects of stronger nonlinearities on AM/PM conversion. The time domain analysis will be simulated to verify if it is better suited for modelling stronger nonlinearities through including the impact of higher harmonics on the output.

Both the frequency domain analysis and the time domain analysis approximations indicate that AM/PM conversion effects can be minimalized by reducing the third-order timing constant (RC_3) and the input frequency in first-order low-pass RC-filter sections. These claims will now be verified through conducting several simulations. An explanation on the way the simulations will be conducted can be found in the Method section, the results are in the Results section.

5 Method

This section will elaborate on the methods that will be used to verify the conclusions extracted from the theory section. Paramount to this verification is the validation of the assumptions used, therefore, the assumptions and approximations made will be summarized first.

5.1 Model assumptions

Consider the approximations that were made:

- Transistor distortion was assumed to be properly modelled by weakly nonlinear circuit expressions.
- All other components of the blocks comprising transceiver systems were deemed sufficiently linear.
- Regarding the equivalent circuit of the heterojunction bipolar transistor:
    - The model presented by Maas et al. in [4] was assumed sufficiently accurate.
    - The parasitics presented in this model were considered neglectable.
    - The collector current amplification was considered to be linear.
    - The nonlinearities of the device's depletion region and junction capacitance were both included in the model of the base-emitter capacitance.
- Regarding the linear approximation of nonlinear effects in first-order low-pass RC-filters:
    - The nonlinear expression for the capacitance was assumed to be properly defined by a time-varying capacitance value $C(t)$ which could be used in linear circuit analysis as C_2 and C_3 were considered sufficiently small in relation to C_1.
    - The input frequency was assumed to be well below the cut-off frequency of the circuit ($RC\omega \ll 1$).
    - Even harmonics were assumed to be suppressed in fully differential circuits.

Verification of the first two assumptions is beyond the scope of this research due to their strong dependence on the choices of the circuit designer; there is a large freedom in configurations, component values and used signal routes. The output of this research will be focussed on developing conclusions that can aid this very design process, but the implementation is left to the circuit designer.

5.2 Approximating weakly nonlinear behaviour in HBTs with RC-circuits

The use of the first-order low-pass RC-circuit with nonlinear capacitor as a representation of the HBT will be verified with simulations. For the RC-circuit, a VerilogA model has been made that describes the nonlinearity of the capacitor through the function $C = C_1 + C_2V_c + C_3V_C^2$, see Figure 12. To extract

the change in phase due to AM/PM conversion, the linear equivalent of the first-order low-pass RC-filter has also been included in the simulations.

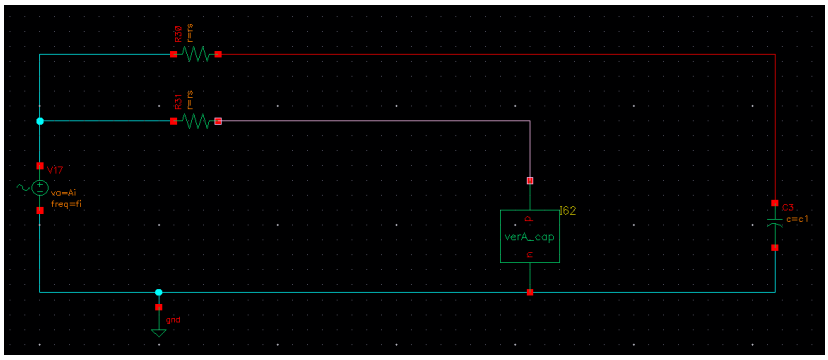

Figure 12: VerilogA model of a nonlinear first-order low-pass RC-filter in parallel with a linear one, in Cadence.

The simulations extracted from the circuit in Figure 12 will be verified with a very accurate model of the HBT from the QUBIC library in Cadence, hereafter to be called QUBIC model. This HBT has been very accurately approximated in this QUBIC model, which is a big advantage when evaluating the mathematical model that should closely resemble nonlinear effects (which are in general much smaller than the linear effects). A downside of using the QUBIC model is the fact that it is not possible to evaluate the behavioural resemblance of the internal nodes of the equivalent circuit in Figure 3, as the transistor can only be measured in its entirety.

In contrast to the simple RC-circuit in Figure 12, the QUBIC HBT model needs biasing for it to properly function. Biasing the transistor can be done in multiple ways. One can set the base-emitter voltage to an appropriate level or force an emitter current. The latter is a way of indirectly setting V_{BE} through the relations $V_{BE} = \frac{kT}{q} \ln\left(\frac{I_C}{I_{C0}}\right)$ and $I_E = \frac{\alpha_{fe}+1}{\alpha_{fe}} I_C$. To aid the proper biasing of the transistor, a tool will be used that conveniently presents useful information on transistor biasing called ProMOST. Since this research primarily considers the internal properties of the transistor on AM/PM conversion, the external circuit is of little importance. Therefore, the biasing will be realized by placing a series DC voltage source across the base-emitter of the capacitor (which can easily be done in theory, but is much more complicated in real circuits). The operating point will be set to $V_{BE} = 0.90\,V$, such that the collector current is set close to 10 mA (this is deemed a proper value for the use of the HBT as a common emitter amplifier), see Figure 13 for the corresponding operating point extracted from ProMOST and Figure 14 for its implementation, including operating point, in Cadence.

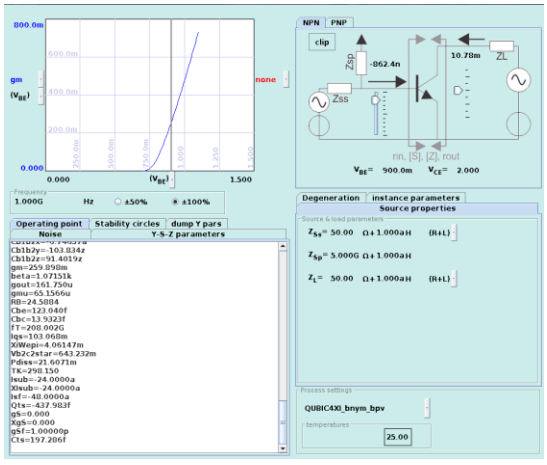

Figure 13: Information on the operating point of the HBT visualized in ProMOST.

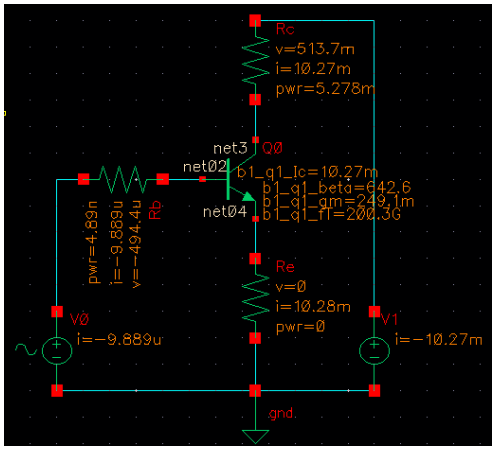

Figure 14: HBT in testbench with bias settings as presented in Figure 13 applied. Rb, Rc and Re have been set to 50, 50 and 0 Ohms respectively.

Important simulations to perform are the above-mentioned DC operating point and transient simulations that enable the evaluation of signal shapes in the time domain. However, most important is the AM/PM conversion that manifests itself within the HBT. If the mathematical model is able to properly model these effects, it can be used to investigate the effects of altering the source impedance and the internal device properties.

As AM/PM conversion effects manifest themselves in nonlinear circuits, simulations that are based on a linearized operating point will not suffice. A suitable simulation method is the periodic steady state analysis (PSS). With a periodic analysis, the circuit is driven with one or more periodic waveforms and the steady-state response is computed. This point is subsequently used for small-signal simulations. This is the reason why the phase of the output will be simulated with a PSS analysis implemented through the shooting method.

In Figure 12, the amplitude dependent phase can be simulated by subtracting the phase of the equivalent *linear* circuit (insertion phase) from the *nonlinear* circuit, which has been placed in parallel. This is not possible for the HBT, as the exact linear equivalent parameters of the circuit are not known. Hence, one has to find other ways of visualizing the AM/PM conversion.

Horst and Cressler have presented a measurement set-up used to visualize AM/PM conversion [7]. They state that measuring the phase at the output under a sweep of the input power will manifest the effects if they are present as 'an ideal device with no AM/PM conversion would show a flat phase response across input powers' [7, p. 2]. This statement has also been verified in more recent research, see for instance [11, p. 42]. Thus, the amplitude dependent phase will be visualized by performing an input power sweep under which the deviation of the phase at the output with respect to its insertion phase value will be determined.

Then, to extract the actual AM/PM conversion values, one has to look at the *change* in phase with respect to the *change* in amplitude. To do so, the derivative of the phase-amplitude expression will be derived and plotted. Since the expressions derived in the 'Theory' section consider the phase and not its change, this plot is of relatively little importance and only gives a minor increase in insight.

Default component values of the RC-circuit in Figure 12 will be established as follows:

- $R_s = 50\ \Omega$
- $C_1 = 318\ fF$, $C_2 = 16\ fF$, $C_3 = 16\ fF$
- $\omega_{cut-off} = \frac{1}{RC_0} = 20\pi \frac{Grad}{s} => f_{Cut-off} = 10\ GHz$

- $f_{in} = 10\ GHz$

Note that C_1 is not expected to exert any influence on the AM/PM conversion effects of the RC-network, only on the insertion phase. Since the insertion phase will be subtracted from the output phase for visualizing the amplitude dependent phase shift, the exact value of C_1 is expected to be of little importance. C_2 and C_3 are harder to estimate, their values have been set to be 20 times smaller than C_1, but question is whether that is a proper representation of the nonlinearities of both the junction capacitance and the depletion region. Therefore, their values will be varied in the simulations.

After the analysis on the ability of the RC-network to be used as an accurate model to analyse the AM/PM conversion in weakly nonlinear systems, an analysis will be performed on the effects extending this circuit has on the accuracy of the model. The proposed extensions of Section 4.7 where an extra resistor will be added first to model the internal base resistance and second to model the diode, will be evaluated.

A value has to be determined for both extra resistors. Since transistors have a low-Ohmic input, the value of the internal base resistance of the HBT is expected to be small. Several researches have looked into the relation of this internal base resistance to other device properties of the HBT, see for instance [12], and show that the value is indeed small. Therefore, the value of the extra resistor after the base will be swept from 0 to 50 Ohms.

The value of the resistor representing the diode can be chosen in a very large range. Large values will show similar results to the RC-network (they are closer to the infinite resistance of the open circuit present there). Smaller values will result in no AM/PM conversion as the nonlinear capacitor will effectively be bypassed with a short-circuit. It will therefore be swept in a relatively wide range; from 0 to 100 $k\Omega$.

The relation between AM/PM conversion and zero-crossings will be made explicit in simulation results by considering the time domain waveforms of the base of the HBT and the capacitor node in the RC-circuit. The data that comprises the waveforms will be exported to another program capable of applying functions to large sets of data, like Excel or MATLAB, so that the timestamps at which the voltage is equal to zero can be extracted. Then, to evaluate the impact of the circuit on the zero-crossings, the difference between the timestamps at the evaluated node and the input should be calculated.

5.2.1 Simulations to perform

The following simulations will be performed to verify the use of a first-order low-pass RC-filter as an equivalent for an HBT circuit to model AM/PM conversion effects:

- Biasing of the HBT will be simulated:
  - DC-operating point
  - Transient simulation for 1 nanosecond of a sinusoid with amplitude of 100 mV applied across the base-emitter and the signal at the collector to check visually for any distortion due to improper biasing.
- Transient simulation at the base of the transistor and at the node between R and C in the RC-section for an input amplitude of 100 mV (limited by bias). This simulation will be compared to the signal applied at the input.
- A PSS simulation on the phase at the base of the HBT for an input amplitude sweep from 100 μV_p to 100 mV_p from which the insertion phase is to be subtracted.
- The derivative of the above plot to show the AM/PM conversion.

- The following simulations on the RC-circuit (and on its extensions as presented in Figure 9 and 10 in Section 4.7 if they prove to be a better representation):
    - Multiple PSS simulations on the phase at the node between R and C in the RC-section (or at the base of the circuits in Figures 9 and 10) for an input amplitude sweep from 100 μV_p to 100 mV_p from which the phase of the linear circuit is to be subtracted:
        - Under a sweep of the values for C_2 and C_3 from 1 fF to the value of C_1 (318 fF), to establish if values can be found that accurately represent the nonlinear depletion region and junction capacitance in a simple model.
        - Under a sweep of the value for C_1 from 1 fF to 5 pF to check the claim that C_1 has no influence on AM/PM conversion, the ratio between C_1 and C_2/C_3 will be kept constant at 1/20.
    - The derivative of the above plots to show the AM/PM conversion.
- Transient simulations will be performed, data will be collected from three differential nodes: the input, the base of the HBT and the nonlinear output of the RC-circuit. The transient simulation will be run for 1 μsecond. The data will be exported to perform data analysis in MATLAB such that the zero-crossing timings can be extracted, refer to Appendix 10.4.3 for the code

5.3 Verifying the use of linear circuit analysis to model nonlinear AM/PM conversion in first-order low-pass RC-sections

The RC-section in Section 5.2 will be altered and then used to conduct simulations for this section. The approximation has been derived with the assumption that it would be applied to differential circuits (resulting in suppression of even harmonics). Therefore, the single-ended RC-section from Figure 8 will be made differential, see Figure 15. Simulations performed on this differential circuit will be compared to purely theoretical curves representing the results from the approximation that has been presented in Section 4.7.

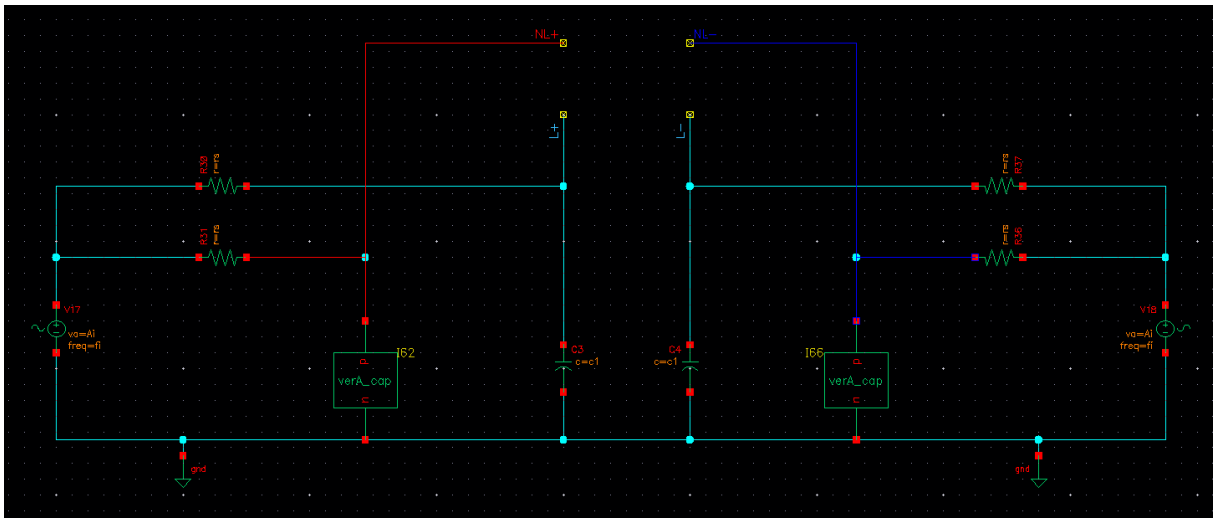

Figure 15: Differential version of the circuit in Figure 8.

Focus will be set to the parameters that together comprise this theoretical approximation: ω_{in}, R and C_3. The influence of R and the capacitance constants of the first-order low-pass RC-filter depicted in Figure 8 will be looked into by sweeping the input amplitude and the before-mentioned constants. Emphasis will be set to the ratio between the nonlinear capacitance constants and the linear one and the influence of the cut-off frequency as these were explicit assumptions. To be able to properly

characterize the influence of the first order capacitance constant on the AM/PM conversion effects, it will therefore be varied in two different methods:

1. C_1 will be varied without varying R_s. This means that the cut-off frequency of the RC-circuit will change. This effect on the cut-off frequency will be included in the discussion of the results.
2. C_1 will be varied and the cut-off frequency will be kept constant. This means that R_s will also change.

The default circuit component values will be identical to those in Section 5.2.

The relation between AM/PM conversion and zero-crossings will be made explicit in simulation results by considering the time domain waveforms of the output nodes in Figure 15. These results will be compared to the theoretical results discussed in Section 4.8.2.

5.3.1 Simulations to perform

The following simulations will be performed to verify the linear approximation to nonlinear AM/PM conversion effects in RC-sections:

- To verify that even harmonics are indeed suppressed in differential circuits, C_3 will be set to zero and the input amplitude will be swept from 5 mV_p to 100 mV_p. A PSS simulation will be performed to visualize the nonlinear component of the phase.
- A PSS simulation will be performed in which C_2 will be set to zero and the input amplitude will be swept from 5 mV_p to 100 mV_p. The curve of the approximation presented in Section 4.7 will be included to enable comparison.
- Multiple PSS simulations will be performed in which C_2 will be set to zero and the input amplitude will be swept from 5 mV_p to 100 mV_p under the following sweeps:
    - A sweep of R_s from 0 to 500 Ω.
    - A sweep of C_1 from 1 fF to 5 pF, the ratio between C_1 and C_3 will be kept constant.
    - A sweep of C_1 from 1 fF to 5 pF, the value of C_3 will be kept constant.
    - A sweep of C_1 from 1 fF to 5 pF in which the cut-off frequency will remain fixed (so R_s will be adjusted to maintain a constant $R_S C_1$ product).
    - A sweep in value of C_3 with respect to C_1, this will be done by defining $C_3 = \frac{C_1}{x}$ and sweeping x from 1 to 50.
- Transient simulations will be performed, data will be collected from three differential nodes: the input, the nonlinear output and the linear output. The transient simulation will be run for 1 μsecond. The data will be exported to perform data analysis in MATLAB such that the zero-crossing timings can be extracted, refer to Appendix 10.4.3 for the code.

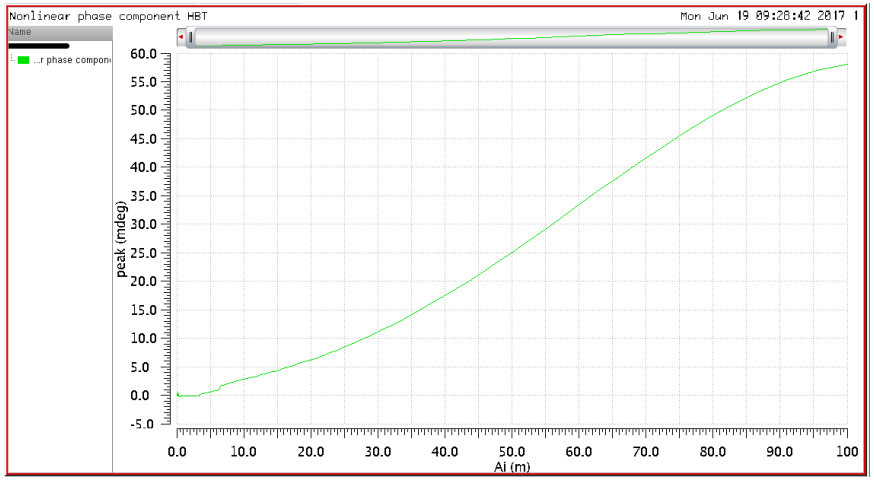

Figure 16: The nonlinear phase component at the base of the HBT under an amplitude sweep showing the dependence of the phase on the amplitude applied at the input.

6 Results

This section contains the results of the simulations performed with Cadence, as proposed in the Method section that have been performed to verify the theory. If intermediate results gave rise to the need for more simulations due to phenomena that had not been anticipated, these have been included here as well. Simulations that are of minor importance to the conclusions of this thesis have been collected in Appendix 10.5, they will be referred to when needed.

6.1 Approximating weakly nonlinear behaviour in HBTs with RC-circuits

The Heterojunction Bipolar Transistor has been biased as proposed in the Method section, see Figure 14. In contrast to the statement in the Method that an input amplitude up to 100 mV_p would still be sufficiently linear, this value has been re-established at 50 mV_p, due to the already stronger nonlinear behaviour beyond an input amplitude of 50 mV_p. The default linear capacitance parameter C_1 has been established at 123 fF, this value represents the HBT better. Please refer to Appendix 10.5.1 and Appendix 10.5.2 for a discussion on both decisions. Note that the phase at the base of the HBT will be evaluated and not at the collector, an explanation for this has been given in Section 4.5.

The next step is looking into the ability of the RC-network to model the effects of AM to PM conversion in HBTs operating in a weakly nonlinear mode. To do so, a plot of the AM/PM conversion in the HBT will be simulated. To this end, consider Figure 16 showing the nonlinear phase component (total phase minus the insertion phase) of the signal at the base under an input amplitude sweep. The sweep has been run from 0 to 100 mV_p input amplitude to check if the claims that the HBT is already operating in a strong nonlinear regime at an input amplitude of 100 mV_p were justified.

Figure 16 shows that for higher input amplitudes the HBT starts manifesting stronger nonlinear behaviour. The squared dependence of the phase on the input amplitude

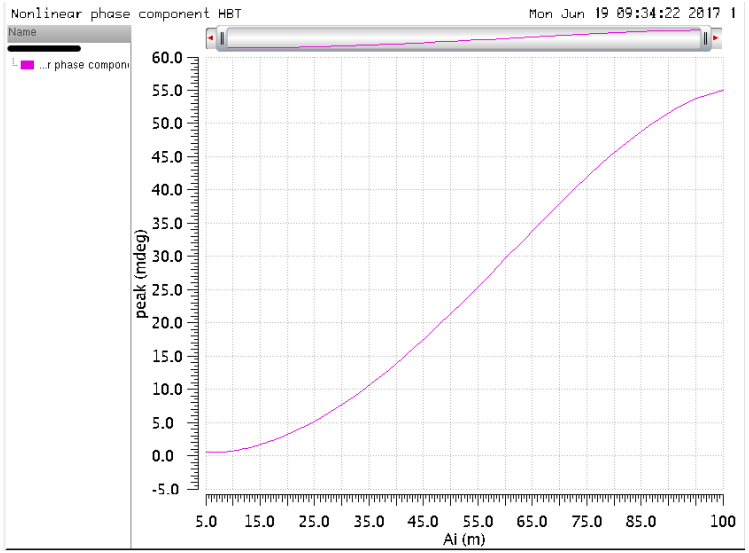

Figure 17: The nonlinear phase component at the base of the HBT, under an input amplitude sweep with increased accuracy settings.

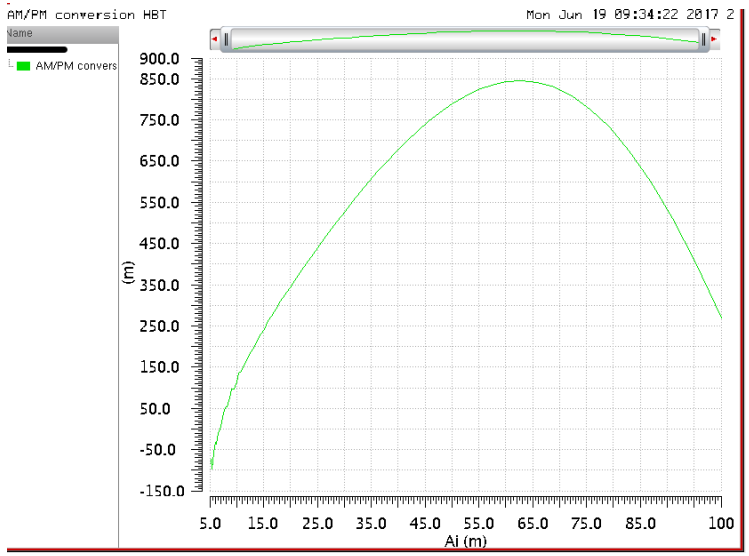

Figure 18: PSS simulation of the AM/PM conversion at the base of the HBT, run from 5 mV to 100 mV.

as presented in Section 4.7 ($\phi(A) = -\frac{R_s C_3 \omega_{in} A^2}{2}$) can no longer be considered to hold when the input amplitude surpasses 50 mV_p (also note that due to the way of plotting, the phase change is positive instead of negative with increasing amplitude). The actual AM/PM conversion can be derived from the nonlinear phase component by taking the derivative with respect to the input amplitude ($\frac{d\phi(A)}{dA} = -R_s C_3 \omega_{in} A$).

To improve the simulations at lower input amplitude values, accuracy of the simulations will be increased; consider the plots of both the nonlinear phase component (Figure 17) and the actual AM/PM conversion (Figure 18) for these revised accuracy settings. For additional discussion on this topic, please refer to Appendix 10.5.3.

Figure 18 already indicates that the relation between amplitude modulation at the input and phase modulation at the base of the HBT cannot be approximated by a linear curve when it is pushed into stronger nonlinear regimes. To visualize what happens when one uses a weakly nonlinear approximation, Figures 19 and 20 have been plotted.

Figures 19 and 20 show that the lower range of the input amplitude sweep (from 0 to ~50 mV_p) can be reasonably approximated with a simplified RC-network when the right values have been chosen for the nonlinear capacitance constant C_3 (the term that maps onto the harmonic), C_2 has been set to zero. However, for input amplitude values surpassing 50 mV_p, the approximation is not accurate and shows a clear mismatch (refer to Figures 19 and 20).

For the component values used in these simulations, a value of 84 fF for C_3 will yield a proper representation of the nonlinear phase component of the HBT for input amplitudes up to 50 mV_p. Since the AM/PM conversion is directly related to the nonlinear phase component through the derivative, it can also be properly modelled with the RC-circuit up to an input amplitude of 50 mV_p.

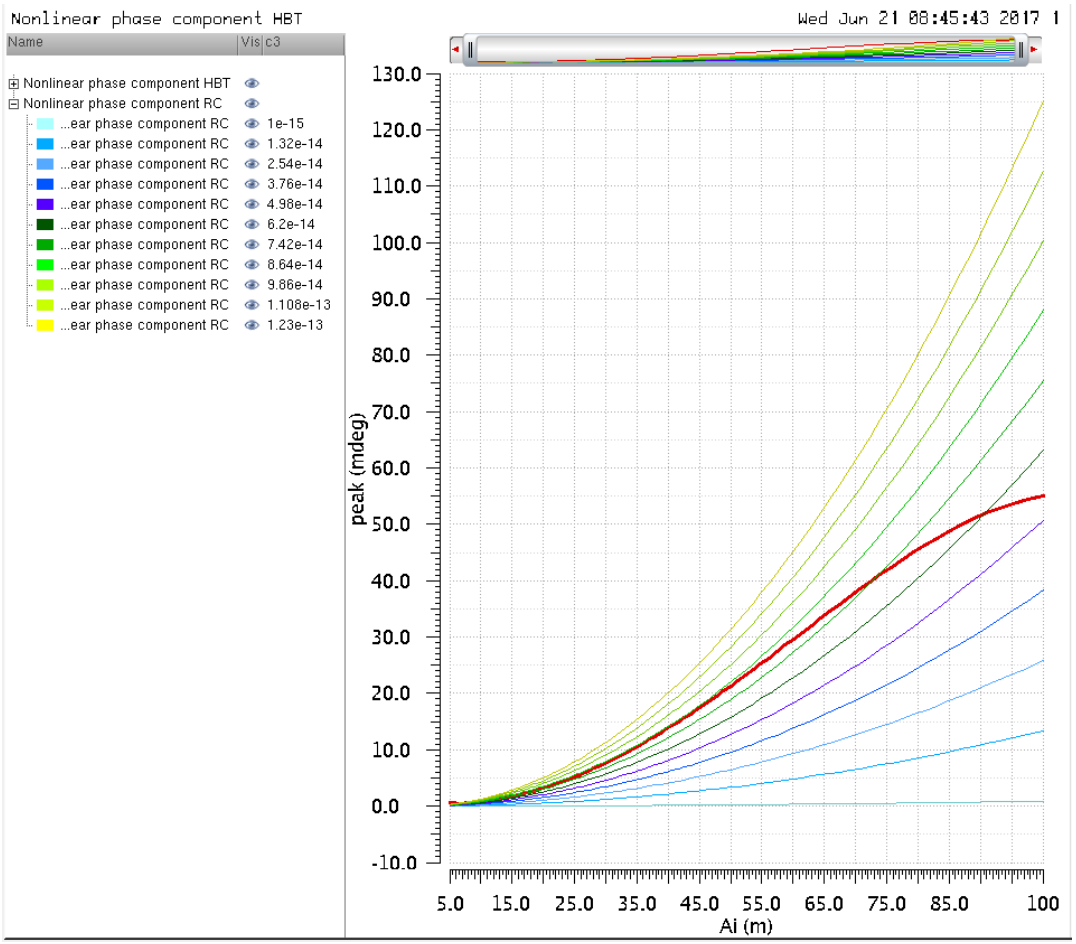

Figure 19: Nonlinear phase component of the RC-circuit under an input amplitude sweep for various values of the third-order nonlinear capacitance constant C_3. The red line indicates the nonlinear phase component of the HBT evaluated at the base.

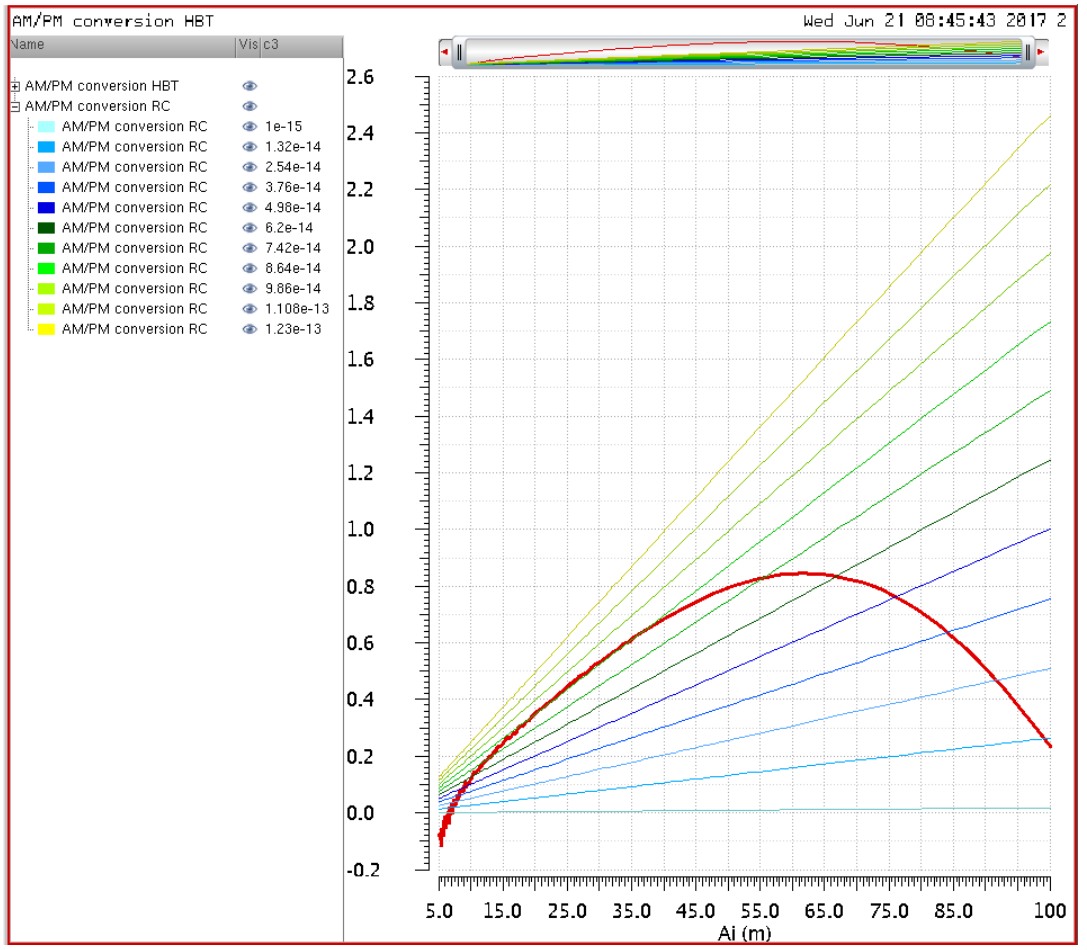

Figure 20: AM/PM conversion of the RC-circuit for various values of the third-order nonlinear capacitance constant C_3. The red line indicates the AM/PM conversion of the HBT evaluated at the base.

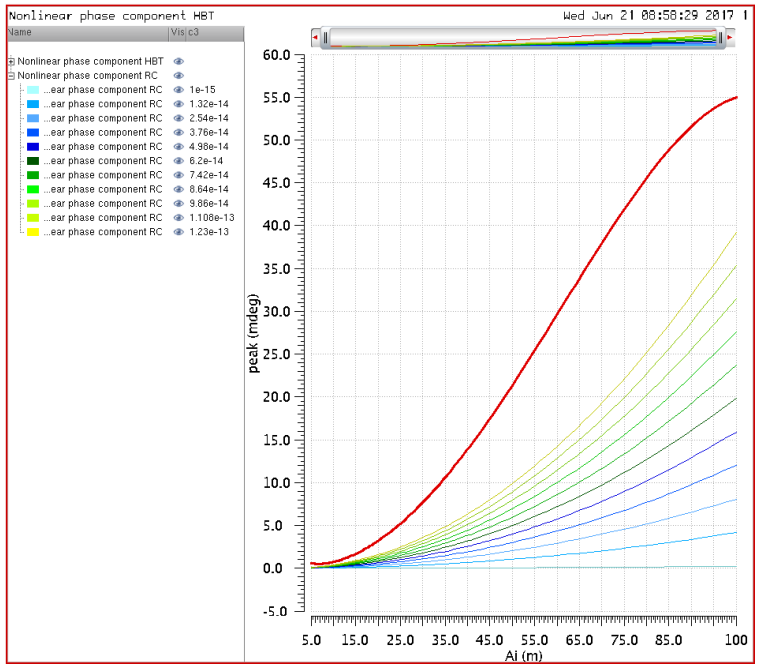

Figure 21: Nonlinear phase component of the RRC-circuit under an input amplitude sweep for various values of C_3. Red line for the values at the base of the HBT.

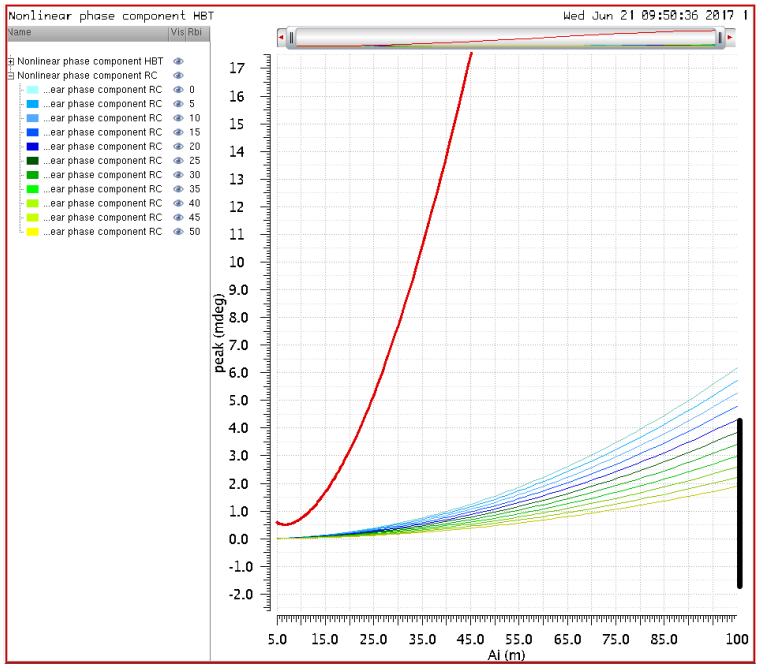

Figure 22: Nonlinear phase component of the RRC-circuit under an input amplitude sweep for various values of R_{bi}. Red line for the values at the base of the HBT.

To see if the simple first-order low-pass RC-circuit can be extended to improve this 'approximation limit' of 50 mV_p, let us consider similar simulations as in Figures 19 and 20 performed on the proposed extensions from Section 4.7 in Figures 21 and 22.

Figure 21 shows the same simulation settings as Figure 19, but the internal base resistance R_{bi} has been set to 50 Ω. One can clearly notice that the curves have been attenuated by the new configuration and that the internal resistance only decreases the cut-off frequency of the circuit and hence reduces the magnitude of the signal that appears across the capacitor. Now consider the effect of this same internal resistance under a value sweep from 0 to 50 Ω when the value of C_3 is kept constant, see Figure 22.

Figure 22 shows that for larger values of R_{bi}, the nonlinear phase component reduces in magnitude and therefore also the AM/PM conversion reduces in magnitude. The quadratic dependence of the nonlinear phase component on the input amplitude does not change (so this curve cannot match the stronger nonlinearities for input amplitudes beyond 50 mV_p either). Extending the first-order low-pass RC-filter with the internal base resistance does not yield a better model to approximate the AM/PM conversion in HBTs.

Next, the effects of modelling the depletion region with an additional resistor placed in parallel with the nonlinear capacitance have been evaluated. Figure 23 shows the AM/PM conversion for a sweep of the values for R_{be}.

Figure 23 shows that a sweep of the value for R_{be} from 0 to 100 $k\Omega$ leads to a transition in value of the AM/PM conversion from being equal to zero to being equal to the general first-order low-pass RC-filter. Including a linear version of R_{be} will therefore only further attenuate the AM/PM conversion which will not lead to better approximations.

Figures 21, 22 and 23 show that the extensions proposed in Section 4.7 do not yield any better results for approximating the AM/PM conversion in the weakly nonlinear

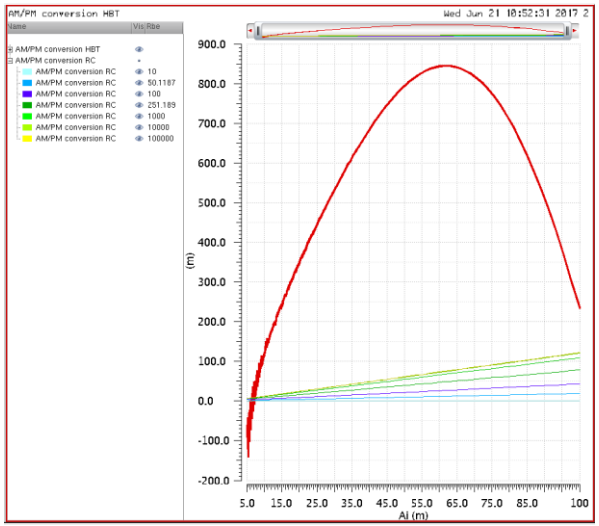

Figure 23: AM/PM conversion in the R(C//R)-circuit under a sweep of R_{be}. The red line gives the AM/PM conversion at the base of the HBT.

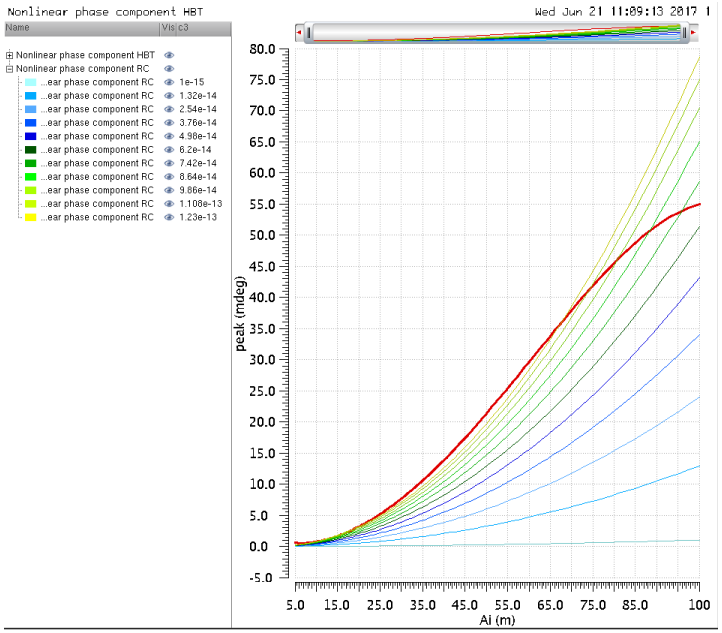

Figure 24: Nonlinear phase component of the RC-circuit under an input amplitude sweep for various values of C_2 and C_3 ($C_2 = C_3$). The red line indicates the nonlinear phase component at the base of the HBT.

regime of the HBT. The Figures show that the additional resistors only further attenuate the nonlinear phase component, something that can also be achieved by reducing the third-order capacitance constant in the original first-order low-pass RC-filter. Thus, since the extensions do not offer anything that cannot be achieved by the simpler first-order low-pass RC-filter, this circuit will be used to analyse the approximations.

Now, one can look into the approximation of the simple RC-circuit below the 'approximation limit', can it be made any more accurate than shown in Figure 19 and 20? For this, consider Figures 24 and 25 for a sweep on the value of C_2 in combination with C_3 (Figures 19 and 20 were based on a sweep of only C_3).

Figures 24 and 25 show that for values of C_2 and C_3 that approach the value of C_1, the effects of both terms start cancelling and the AM/PM conversion magnitude no longer increases. To verify this claim, an additional simulation has been performed in which only C_2 has been swept, see Figure 26 on page 30.

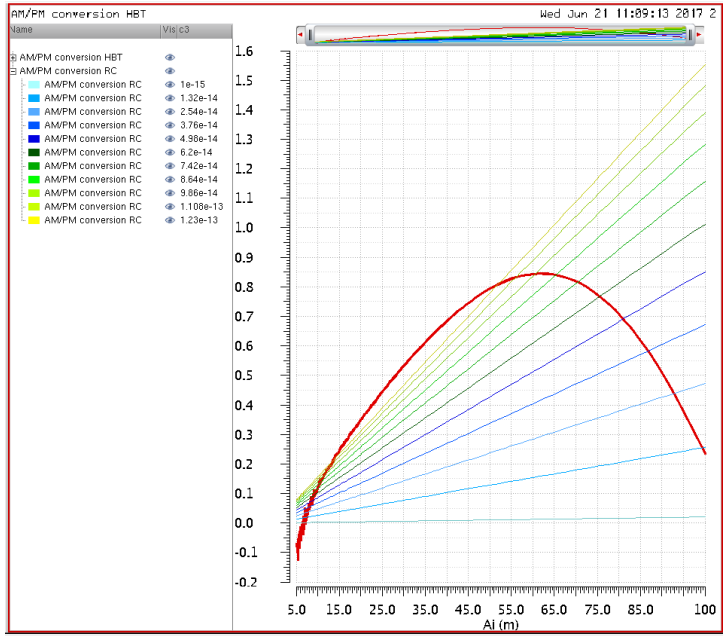

Figure 25: AM/PM conversion of the RC-circuit for various values of C_2 and C_3 ($C_2 = C_3$). The red line indicates the AM/PM conversion at the base of the HBT.

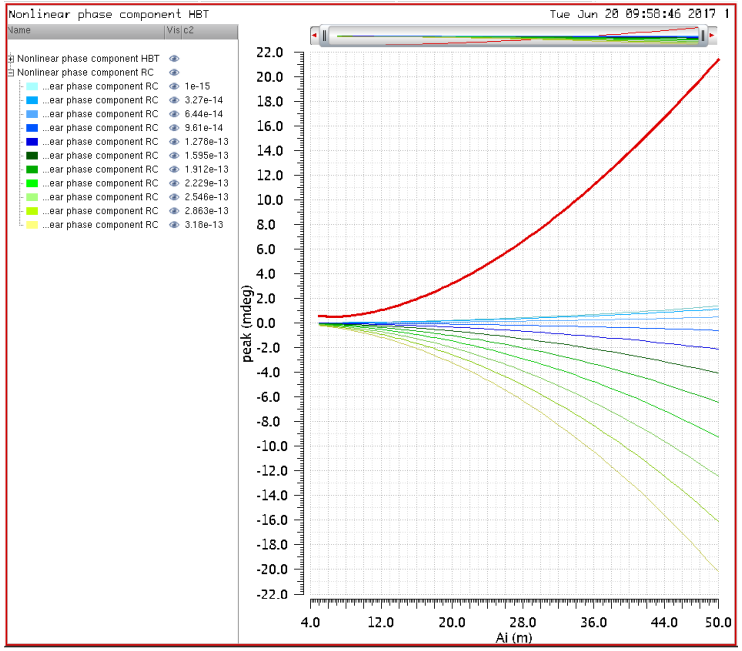

Figure 26: Nonlinear phase component of the RC-circuit under an input amplitude sweep for various values of C_2 when C_3 has been set to zero. Red line shows the nonlinear phase component at the base of the HBT.

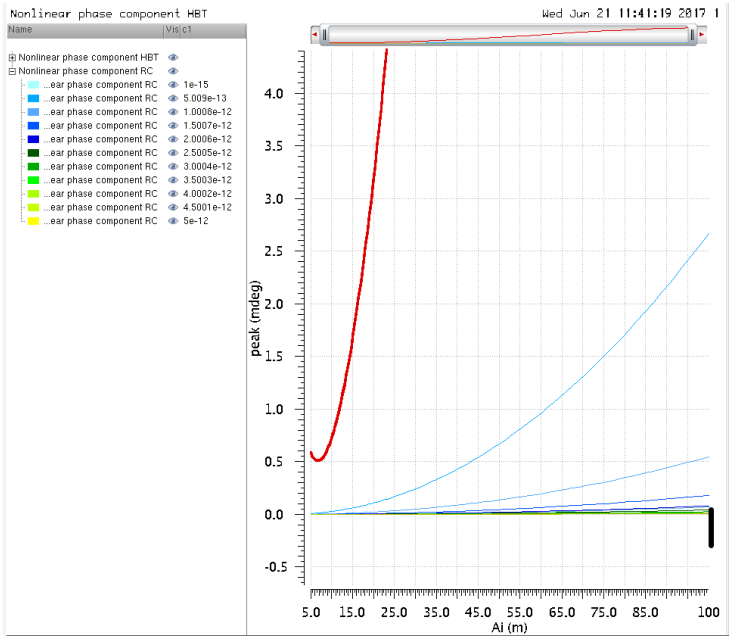

Figure 27: Nonlinear phase component of the RC-circuit under an input amplitude sweep for various values of C_1. Red line shows the nonlinear phase component at the base of the HBT.

Figure 26 shows that the contribution of the second-order nonlinear term to the nonlinear component of the phase under an input amplitude sweep is of opposed sign. For increasing values of C_2 and C_3, the increase of C_2 is stronger than that of C_3, resulting in cancellation of both terms, explaining the results in Figures 24 and 25.

Note that most high-performance RF circuits are differential and that contributions caused by even harmonics in such odd-symmetric circuits are cancelled out. Mismatches and nonidealities in differential circuits will cause some influence of even harmonics to remain, but these will be small compared to the contributions of the other terms, this statement will be revisited in Section 6.2.

Figure 27 shows a sweep of value of C_1. To be able to evaluate it without evaluating the relative impact of the nonlinear constants, C_2 and C_3 have been kept constant at a value of $\frac{C_1}{20}$.

One can notice the decline in the magnitude of the nonlinear phase component for increasing values of C_1, in contrast to the statement in the method section that C_1 was not expected to exert any influence. Since C_1 is a linear constant, it can only indirectly cause this change in magnitude of the nonlinear phase component.

Increasing C_1 leads to a reduction of the influence of the nonlinear constants; the cut-off frequency of the circuit changes and, as a result, the magnitude of the signal across the terminal of the capacitor will be attenuated beyond a certain threshold. In this case where the input frequency is 10 GHz and $R_s = 50\ \Omega$, this value is equal to $\frac{1}{2\pi \cdot 50 \cdot 10^{10}} = 318\ fF$.

The results presented up to now have been based on the fundamental frequency; the plotting techniques used have only evaluated the phase at this single frequency. To verify the resemblance between the behaviour of the HBT and the RC-circuit in the time-domain, the zero-crossings have been evaluated. Time domain waveforms have been evaluated using Cadence to find their zero-crossing values. These values

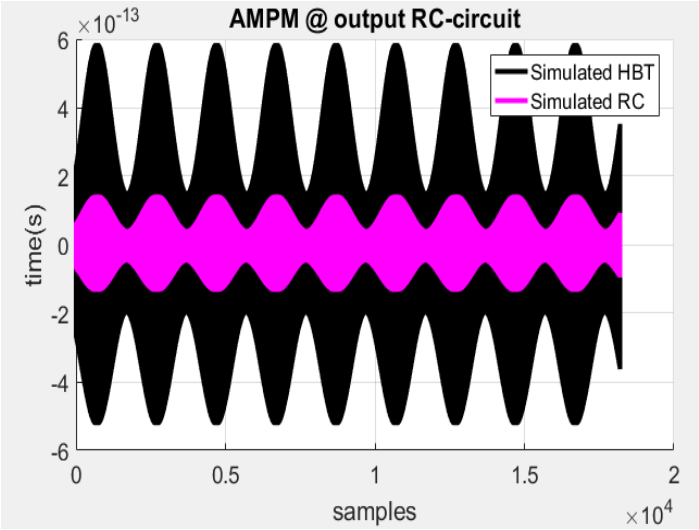

Figure 28: Deviation in zero-crossings for the HBT and the RC-circuit. Capacitance values of the RC-circuit have been established as follows: $C_1 = 123\ fF$, $C_2 = 84\ fF$ and $C_3 = 84\ fF$. Input amplitude is 50 mV_p.

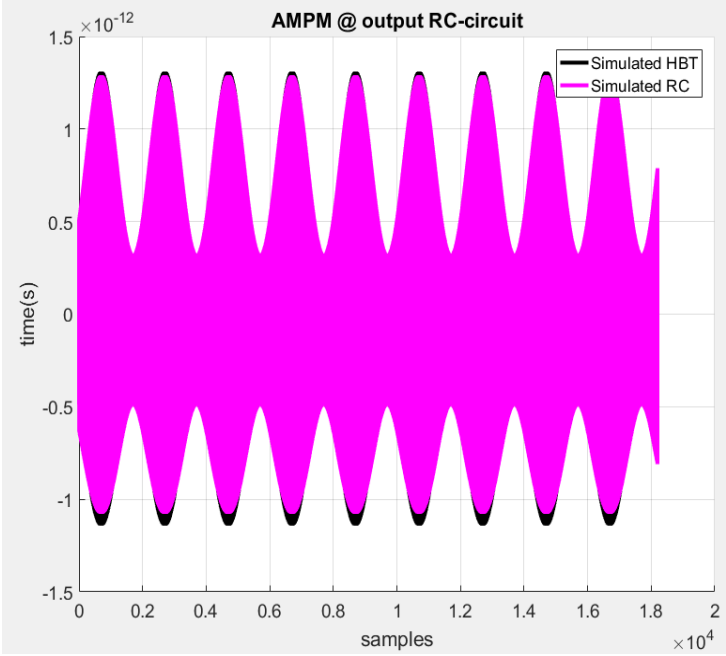

Figure 29: Deviation in zero-crossings for the HBT and the RC-circuit. Capacitance values of the RC-circuit have been established as follows: $C_1 = 123\ fF$, $C_2 = 360\ fF$ and $C_3 = 360\ fF$. Input amplitude is 100 mV_p.

have been visualized using a MATLAB-script, please refer to Appendix 10.4.3 for the code.

As an initial guess, the values that properly modelled the HBT in the weakly nonlinear regime in the frequency domain evaluation of the phase of the fundamental, have been used in this evaluation of the zero-crossings in the time domain. However, the effects of C_2 should now also be taken into account, since individual parameters of the HBT cannot be controlled. 28 shows the deviation in zero-crossings for these capacitance values ($C_1 = 123\ fF$, $C_2 = 84\ fF$ and $C_3 = 84\ fF$) and an input amplitude value of 50 mV. The contribution of C_2 causes the deviation of every alternating zero-crossing to change sign due to the sinusoidal dependence of the deviation in zero-crossings on the input amplitude (the contribution of C_3 is being squared as a result of which it does not change sign). Making the circuit differential will eliminate this contribution, resulting in the fact that the deviation in zero-crossings will follow only one side of the envelope that modulated the signal (this will be treated at the end of Section 6.2).

Figure 28 shows that the RC-circuit exhibits weaker nonlinearity than the HBT (the magnitude of the peaks of the deviation in zero-crossings is smaller). Since the used value for C_3 of 84 fF was a proper approximation in the frequency domain when evaluating the fundamental frequency, this means that the contribution of higher harmonics is significant and that the used value of C_3 is too low to properly include them in the time domain waveform.

An increase of C_2 and C_3 to 360 fF yields a much better approximation. Appendix 10.5.3 contains several plots conducted with these capacitance values for different input amplitudes. To check if the time-domain analysis of the zero-crossings can be used for a larger input amplitude than the frequency domain analysis, the quality of the approximation has been evaluated at several amplitudes. The plots in Appendix 10.5.3 show that the time domain analysis of the zero-crossings can be used up to a rough 100 mV_p as opposed to the 50 mV_p of the frequency domain analysis. At 100 mV_p input amplitude, and for values that are larger than that, the deviation in zero-

crossings becomes larger in the HBT than those in the RC-circuit, see Figure 29. This trend continues for increasing input amplitude.

The Figures presented in this section of the results have shown that a first-order low-pass RC-section can effectively approximate AM/PM conversion of the fundamental frequency in an HBT operating in the weakly nonlinear regime, but that this approximation is limited to a certain value of the input amplitude (for this case roughly 50 mV_p). When the input amplitude becomes too large, the stronger nonlinear behaviour of the HBT cannot be effectively modelled with a frequency domain analysis of the AM/PM conversion evaluated at the fundamental frequency in the RC-circuit.

The results on the time domain evaluation of the zero-crossings have shown that the inclusion of higher harmonics enables a larger input amplitude range to be covered by the simplified RC-circuit model of the HBT. Through evaluation of the AM/PM conversion effects by considering the related dependence of this phenomenon on the deviation in zero-crossings, the RC-circuit was found to properly model the HBT up to an input amplitude of 100 mV_p for these particular circuit values.

The next section will contain an analysis on what gives rise to the AM/PM conversion effects in this RC-circuit. The parameters that exert influence on the AM/PM conversion effects will be identified and their relation will be characterized such that the results can be used to synthesize better transceiver systems.

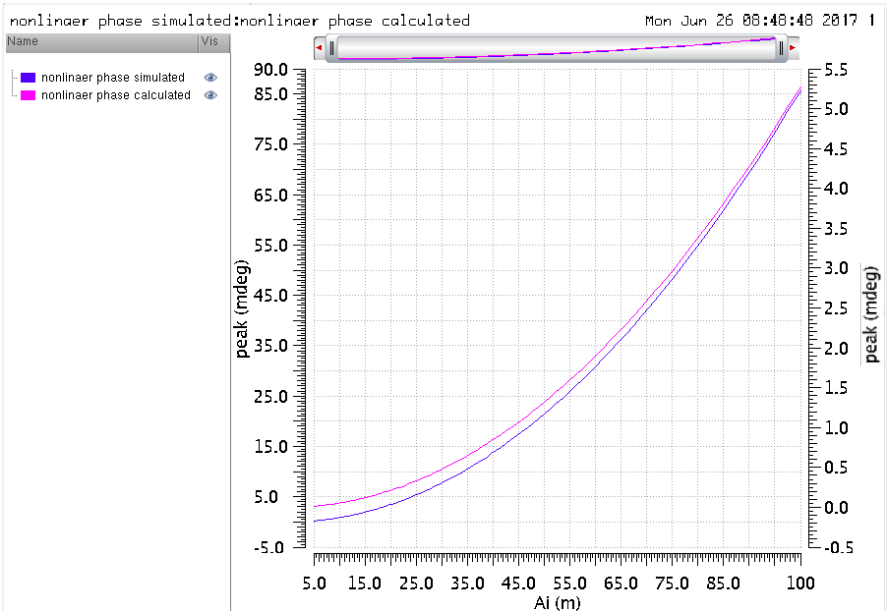

Figure 20: Nonlinear phase component of the RC-circuit ($C_3 = 84\ fF$). The value of the simulated curve can be read on the left y-axis, the value of the calculated curve on the right y-axis.

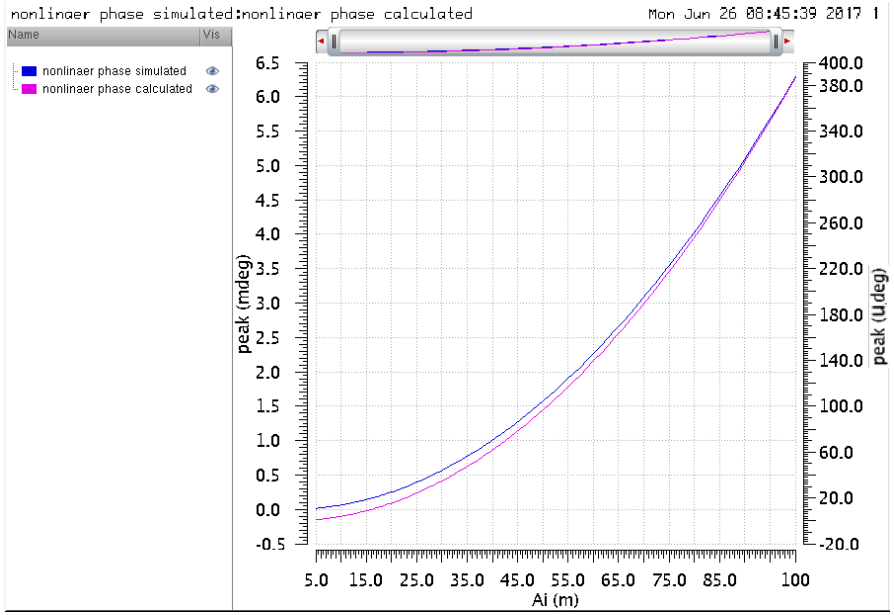

Figure 31: Nonlinear phase component of the RC-circuit ($C_3 = C_1/20\ fF$). The value of the simulated curve can be read on the left y-axis, the value of the calculated curve on the right y-axis.

6.2 Characterizing AM/PM conversion in first-order low-pass RC-sections

The previous section has shown that the simple first-order low-pass RC-filter can be used to describe the AM/PM conversion effects in HBTs operating in a weakly nonlinear mode. To verify the mathematical characterization of the AM/PM conversion in first-order low-pass RC-sections (as presented in Section 4.7) the results of the simulations from the Method section will be discussed here.

As mentioned in the Method, the RC-circuit will be made differential. Simulations have been conducted to verify that the influence of C_2 will be suppressed in differential circuits. This turned out not to be the case due to issues with the solver in Cadence. Please refer to Appendix 10.6 for an analysis on this problem. For the remainder of the results, C_2 has been set to zero.

A simulation has been conducted with the capacitor values that were found to be a proper match to the QUBIC model of the HBT as discussed in Section 6.1: $C_1 = 123\ fF, C_2 = 0\ F$ (differential circuit), $C_3 = 84\ fF, R_s = 50\ \Omega, f_{in} = 10\ GHz$. The approximation has been included in the same plot to enable proper comparison, see Figure 30.

Figure 30 shows that the shape of the approximation properly resembles the behaviour simulated with the VerilogA model, clearly showing the quadratic amplitude dependence in both curves. However, the phase magnitudes are not equal: they differ with a factor of about 16: the magnitude of the approximation is lower than the magnitude of the simulation. The nonlinearities are stronger than anticipated; to check if the approximation that C_3 should be small in comparison to C_1 has been violated (84 fF with respect to 123 fF might be too large), C_3 will now be set to $\frac{C_1}{20}$, see Figure 31.

Figure 31 shows similar results as Figure 30; again, the shape of the curve of the approximation is a good match to the simulation, but the phase magnitudes differ

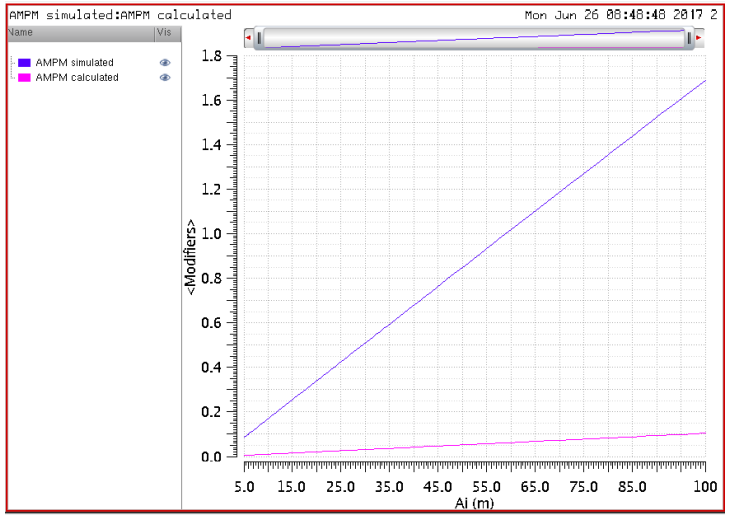

Figure 32: AM/PM conversion of the RC-circuit ($C_3 = C_1/20\,fF$), plot shows both the simulated results and the calculated results. The y-axis is in $10 \cdot \Delta\phi/\Delta A$.

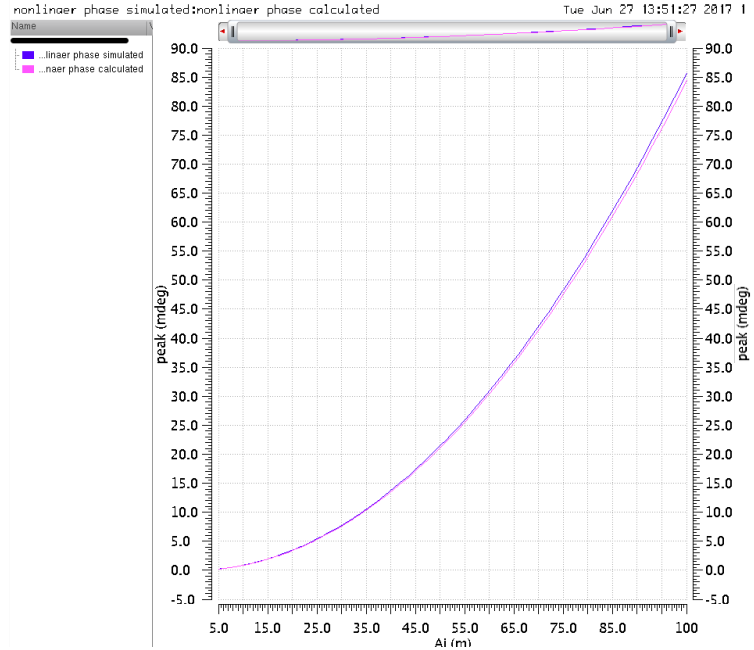

Figure 33: Nonlinear phase component of the RC-circuit ($C_3 = 84\,fF$) after correction to the calculated curve has been applied. The value of the simulated curve can be read on the left y-axis, the value of the calculated curve on the right y-axis.

with roughly the same factor of 16. This has a major impact on the quality of the approximation of the AM/PM conversion effects, see Figure 32.

The reason for the mismatch in magnitude should be found in the way the approximation and the assumptions that were made in that process have been derived. The assumption that the circuit should operate far below the cut-off frequency has not been violated ($f_c = \frac{1}{2\pi RC_1} = 25{,}9\ GHz$, 2.5x higher than the input of $10\ GHz$). The second assumption regarded the relative impact of the nonlinearities on the linear operation of the circuit (C_3 should be small in comparison to C_1). Figures 30, 31 and 32 show that the nonlinearities of the RC-network have been linearized too strongly in the approximation. Even for the case in which C_3 is 20 times smaller than C_1, the approximation does not hold properly.

For the remainder of the simulations, the factor of 16 will be added to the calculated curves through increasing C_3. The exact reason for the difference in magnitude will not be looked into due to the limited time available. It is more important that the approximation *can* be adjusted in such a way that it is capable of modelling the behaviour of the RC-circuit, than that all the values have been accounted for, but the approximation fails to properly match the simulations. Refer to Figure 33 for the calculated and simulated nonlinear phase components after this proposed correction.

To verify if the approximation can be used to describe the impact of the circuit properties on the AM/PM conversion effects (albeit the quantitative match has been 'forced' by including a manual factor), the various parameters will be swept as proposed in the Method section. The approximation indicates that an increase in either R_s, C_3 or ω_{in} should increase the magnitude of the AM/PM conversion effects, these claims will now be verified.

Figure 34 shows the nonlinear phase component for various values of R_s (C_3 has been set back to the best matching value of 84 fF). To better visualize the impact of R_s, each of these curves will be evaluated at $A_i = 50\ mV_p$, the corresponding values

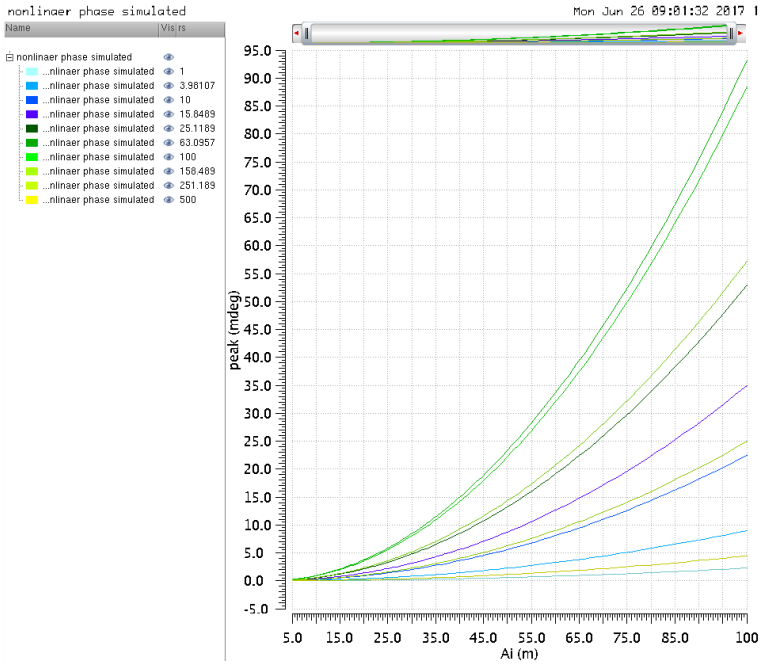

Figure 34: Simulated nonlinear phase component of the RC-circuit under a sweep of R_s.

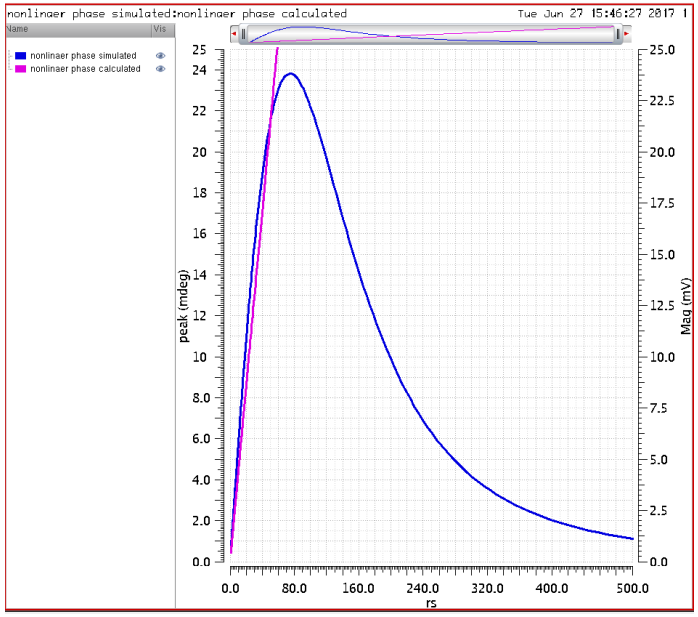

Figure 35: Value of the nonlinear phase component of the RC-circuit evaluated at $A_i = 50\ mV_p$ under a sweep of R_s. The calculated approximation has been included.

of the nonlinear phase will then be plotted against R_s, see Figure 35. This plotting technique will also be used to evaluate the other parameters. The approximation has also been included in this plot for comparison purposes.

According to the approximation from Section 4.7, the dependence of the nonlinear phase on the amplitude should become stronger for larger values of R_s. It is clear that the nonlinear phase component (and thus indirectly the AM/PM conversion effects) cannot be effectively approximated with this approximation for the entire sweep range. A probable cause for this is that one of the two assumptions was violated and hence the approximation can no longer be deemed valid. The assumption that the input frequency would be far below the cut-off frequency appears to hold for lower values of R_s, but not for higher values. Take for instance the lower bound of the parameter sweep performed in Figure 35:

$$1\ \Omega \cdot 123\ fF \cdot 20\pi \cdot 10^9 \frac{rad}{s} \approx 0.0077\ rad$$

This value is indeed much lower than 1 and hence, the approximation that the AM/PM conversion effects will linearly increase with an increase in R_s holds. However, already at $R_s = 129\ \Omega$ will $RC(t)\omega_{in}$ be equal to 1, from which can be concluded that the approximation is not valid. This can be seen in Figure 35, as the effect of AM/PM conversion effects decreases for increasing R_s if R_s is larger than $80\ \Omega$ (at the cut-off frequency, the signal has already been attenuated with a factor 2, therefore this value is lower than the mentioned $129\ \Omega$).

Why does an increase in R then give a decrease in AM/PM conversion effects? A plausible explanation is the fact that beyond $129\ \Omega$, the cut-off frequency is smaller than the input frequency. A result of this is that the input signal will be attenuated by the low-pass nature of the circuit. A smaller signal will appear across the capacitor terminals and hence the impact of the capacitor's nonlinearities will be smaller. To illustrate this, the value of the cut-off frequency for several instances in the sweep of R_s will be compared to the nonlinear phase component, see Table 1.

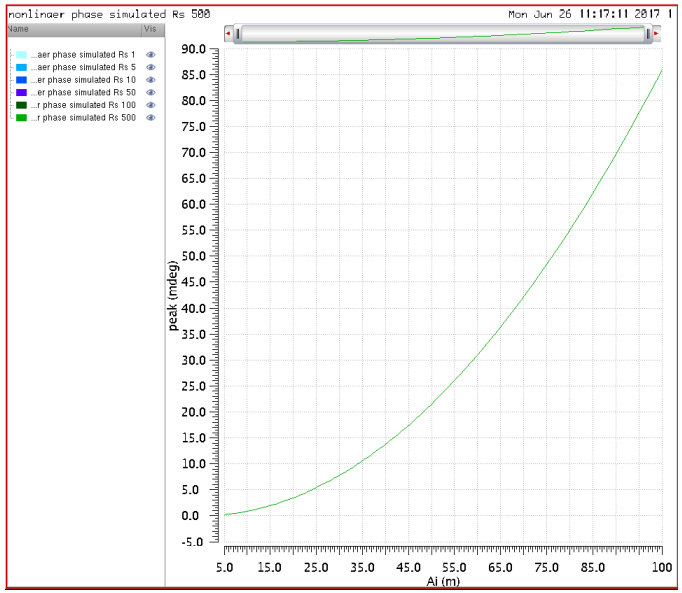

Figure 36: Nonlinear phase component of the RC-circuit for various values of R_s when the cut-off frequency has been kept constant.

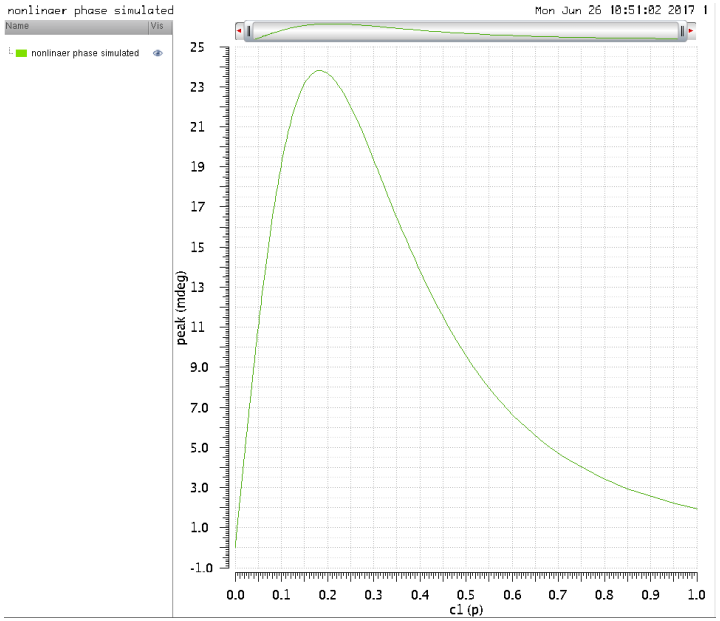

Figure 37: Nonlinear phase component of the RC-circuit evaluated at 50 mV under a sweep of the value of C_1.

Table 1: Table containing the link between a value of R_s and its corresponding nonlinear phase component, cut-off frequency and third-order timing constant.

R_s [Ω]	Nonlinear phase component for $A_i = 50\ mV_p$ [mdeg]	Cut-off frequency [GHz]	R_sC_3 [fs]
1	0.570	1294	84
5	2.87	259	420
10	5.60	129	840
50	21.5	25.9	$4.20 \cdot 10^3$
100	22.1	12.9	$8.40 \cdot 10^3$
500	1.12	2.59	$4.20 \cdot 10^4$

Table 1 shows that for a cut-off frequency that is lower than the input frequency, the nonlinear phase component starts decreasing under increasing R_s. In the case that the cut-off frequency is kept constant, the value of R_s has no impact on the magnitude of the AM/PM conversion effects (consider that RC_3 then stays constant in the approximation), see Figure 36.

A sweep of the first-order capacitance constant as shown in Figure 37 shows similar behaviour as in Figure 35. The explanation on Figure 35 can be extended to Figure 37 as also the first-order capacitance constant determines the cut-off frequency.

Figure 38 shows the nonlinear phase component at an input amplitude of 50 mV, when the value of C_3 is fixed.

One can notice a steady decline in the nonlinear phase component as C_1 increases, this is due to the fact that the ratio between C_1 and C_3 becomes larger and hence the relative impact of the third-order nonlinearity constant on the total capacitance becomes smaller. It is a clear indication that only the third-order constant gives rise to AM/PM conversion effects. The impact changing C_1 has on AM/PM conversion is governed by the changes in ratio between C_1 and C_3, and the fact that the cut-off

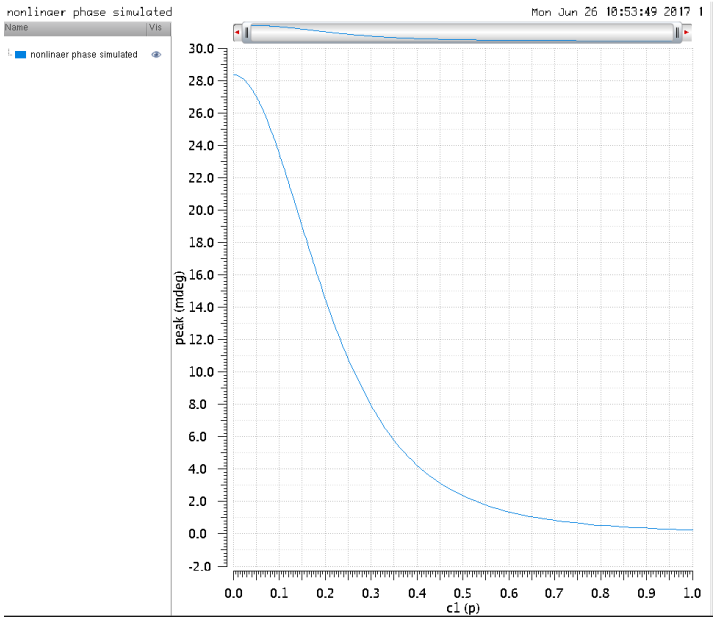

Figure 38: Nonlinear phase component of the RC-circuit evaluated at 50 mV under a sweep of C_1 when C_3 has been kept constant.

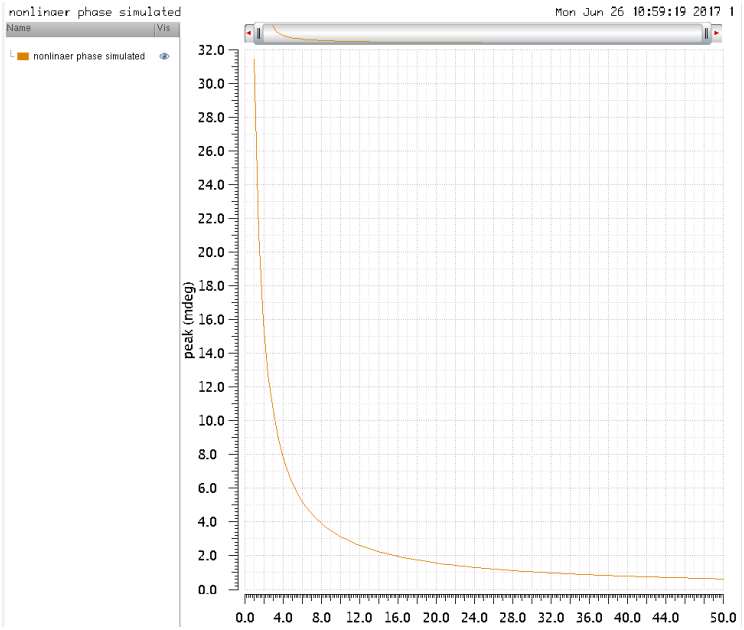

Figure 39: Nonlinear phase component of the RC-circuit evaluated at 50 mV under a sweep of the ratio between C_3 and C_1. The x-axis shows the value of r in the expression $C_3 = C_1/r$.

frequency of the circuit changes. To illustrate this point, consider Figure 39 in which the ratio between C_1 and C_3 has been swept. C_3 has been defined as $\frac{C_1}{r}$, in which case r has been varied from 1 to 50.

Figure 39 shows that a small value for r, and thus a value for C_3 that is close to C_1, yields a much larger magnitude for the nonlinear phase component of the RC-circuit than a large value for this ratio yields.

Next to the constants of the capacitor and the source resistance, the input frequency is also expected to exert influence on the AM/PM conversion magnitude. According to the approximation from Section 4.7, an increase in input frequency should result in an increase in the AM/PM conversion (derivative of the nonlinear phase component with respect to amplitude). Figure 40 on page 38 shows the nonlinear phase component under an input amplitude sweep for several values of the input frequency.

One can derive from the Figure that the cut-off frequency again plays a major role. For the component values used to conduct the simulations, the cut-off frequency is equal to $f_c = \frac{1}{2\pi R_s C_1} = 25{,}9\ GHz$. Up to a value of 20 GHz, the increase in frequency at the input leads to an increase in the nonlinear phase component at the output of the RC-circuit, as the approximation also indicated. Beyond this value of 20 GHz, the input frequency is close to or higher than the cut-off frequency of the circuit. This means that the low-pass nature of the circuit will attenuate the magnitude of the signal that will appear across the terminals of the capacitor and hence also the impact of the nonlinearities on the circuit behaviour.

The simulations presented in the Figures of this section show that if the input frequency is below the cut-off frequency of the circuit, the AM/PM conversion in the first-order low-pass RC-filter can be reduced by minimalizing either the values of ω_{in}, R_s or the value of C_1. If the input frequency is close to the cut-off frequency or beyond it, the AM/PM conversion effects can be reduced by further lowering the cut-off frequency by increasing R_s or C_1, or by increasing the input frequency ω_{in}.

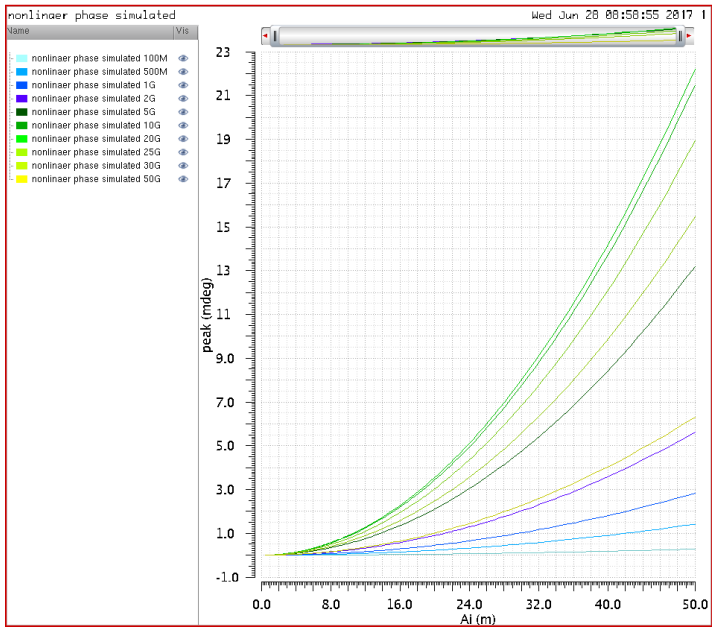

Figure 30: Nonlinear phase component of the RC-circuit for various values of the input frequency f_{in}. The legend shows the value of each curve in Hz.

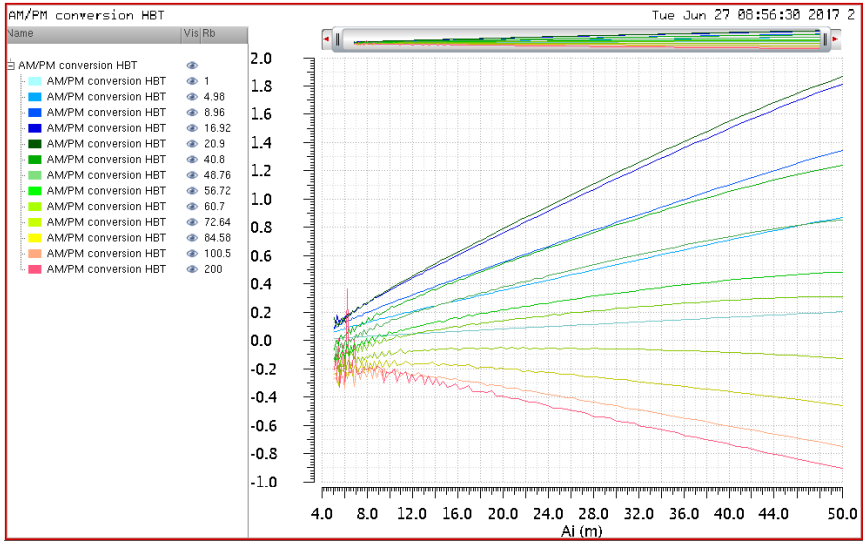

Figure 41: AM/PM conversion magnitude from the input to the base of the HBT for various values of R_b. The legend shows the values for R_b in Ω. The y-axis is in $\Delta\phi/\Delta V$.

Note, however, that lowering the cut-off frequency will also negatively affect the signal at the base and that the process of reducing AM/PM conversion will then become a trade-off between the influence of nonlinearities and the magnitude of the transferred signal.

On a lower level, the AM/PM conversion effects can be reduced if the impact of the nonlinear capacitance constant can be reduced. If the internal properties of the circuit can be altered in such a way that the nonlinearities can be reduced, the AM/PM conversion effects will also reduce.

Section 6.1 has shown that the AM/PM conversion in an HBT operating in a weakly nonlinear regime can be approximated with the first-order low-pass RC-filter if the correct values for the constants have been chosen. This section has shown what parameters influence the magnitude of the AM/PM conversion effects in first-order low-pass RC-filters and how these parameters can be altered to reduce the effects. However, one has to be careful with extending the conclusions from this Section by applying them to the HBT as the RC-circuit is a great simplification of the internal behaviour of the HBT. By altering circuit properties of the HBT, the approximations on the nonlinearities of the model of the HBT (discussed in Section 4.5) that were summarized in Section 5.1, might be violated.

Consider for instance a sweep of the source resistance in the differential version of the HBT circuit in Figure 14. Simulations in this Section have shown that for the RC-circuit this would mean that as long as the input frequency is smaller than the cut-off frequency, an increase in R_s will lead to an increase in AM/PM conversion effects. As soon as the input frequency is higher than the cut-off frequency, an increase in R_s will lead to a decrease in AM/PM conversion effects. The results of this sweep for the AM/PM conversion at the base of the HBT have been depicted in Figure 41.

Figure 41 indeed shows that under an increase of R_b (the equivalent of R_s in the RC-circuit) the AM/PM conversion effects first increase and then decrease. However, the turn-over point occurs at a much lower value (~20 Ω) than the RC-circuit

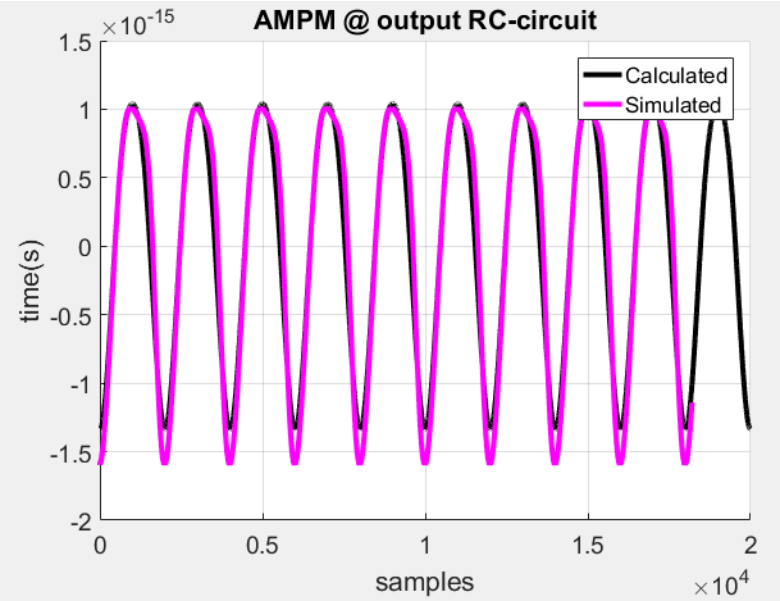

Figure 42: Deviation in zero-crossing values at the output of the RC-circuit for the simulated values (purple line) and the calculated values (black line).

simulations indicate. It is a clear indication that the conclusions drawn in this section on the RC-circuit cannot simply be extended to the HBT.

Further research should be conducted to verify to what extend the conclusions drawn on the simulations performed on the RC-circuit extend to the circuit containing the HBT, and transceiver systems in general.

Zero-crossings

In addition to the frequency based analysis that has been conducted to characterize AM/PM conversion in first-order low-pass RC-filters, a time-domain based analysis has been conducted. The theoretical approximation of the zero-crossings as presented in Section 4.8.2 has been plotted using Mathematica. This plot has been exported to MATLAB in which it has been compared to the zero-crossings of the time-domain simulations conducted on the RC-circuit, see Figure 42.

Figure 42 shows that the approximation contains a linear signal, which does not entirely approximate the nonlinearly distorted simulations. Also, the magnitude of both signals varies slightly which is due to the fact that C_3 is still relatively large with respect to C_1.

7 Conclusion

To synthesize better transceiver systems, the effects of nonlinearities have to be reduced. AM/PM conversion is one of these nonlinearities that leads to unwanted deviations of the phase in transceiver systems. Therefore, modelling of these effects is important for the development of better transceivers, but AM/PM conversion effects are nonlinear and only arise in dynamic nonlinear systems, requiring complex modelling techniques. The conducted research has focussed on characterizing these effects in transceiver systems containing HBTs through simplified models and analyses based on linearized circuit analysis methods to increase insight in AM/PM conversion effects.

A first-order low-pass RC-circuit with a nonlinear capacitor has been presented as a simplified equivalent circuit to the HBT for modelling of AM/PM conversion effects. Both a frequency domain analysis and time domain analysis have been executed to characterize the AM/PM conversion effects in this simplified RC-circuit after which the impact of circuit parameters on the effects has been identified. To deepen insight, several simplifications and assumptions have been introduced in both analyses; their impact on the model accuracy has been considered.

A frequency domain analysis has been conducted to characterize the nonlinear phase component of the fundamental frequency that depends on the input amplitude. Limiting this analysis to the fundamental only, restricts the use of the model to linear and weakly nonlinear systems. Simulations have shown that the frequency domain analysis performed on the RC-circuit can accurately model the AM/PM conversion of an HBT, but that this model is only valid for small input amplitude values in which the HBT can be considered to operate in the weakly nonlinear regime. For the values used in the simulations of this report, this 'approximation limit' was established at an input amplitude value for the small signal of 50 mV_p.

For larger input amplitude values, the time domain analysis is better suited as it includes the impact of higher harmonics on the time domain waveform. Through evaluating the deviation in zero-crossings due to the modulation of amplitude at the input, the AM/PM conversion in the HBT has indirectly been modelled with the same first-order low-pass RC-filter with nonlinear capacitor. The inclusion of higher harmonics has considerably improved the range of the input amplitude for which the model is a proper representation of the behaviour of the HBT when it comes to AM/PM conversion through the evaluation of zero-crossings in the time domain. In this analysis, the 'approximation limit' has been established at an input amplitude for the small signal of 100 mV_p.

Theoretical analysis in both the frequency and time domain indicated that the AM/PM conversion effects in the first-order low-pass RC-filter could be reduced by reducing either the value of the resistor (R_s), the value of the third-order nonlinear capacitance constant (C_3) or the input frequency (ω_{in}). Simulations have verified these claims, but have also shown that the cut-off frequency plays a major role in the accuracy of the theoretical approximations and that the impact of R_s, C_3 and ω_{in} on the magnitude of the AM/PM conversion effects reverses when ω_{in} is larger than the cut-off frequency.

Additional simulations have been conducted that have shown that the conclusions extracted from the simulations on the first-order low-pass RC-filter cannot be directly mapped onto the HBT. Further research will be required to precisely characterize the relation between these conclusions and the behaviour of the HBT.

8 Discussion

This report has covered the answer to the research question, this section will reflect on the steps that have been taken to arrive at this answer.

A model has been presented that is a simplification of the behaviour of a complex heterojunction bipolar transistor (HBT). This model aims at simplifying the complex nature of the nonlinearities that cause AM/PM conversion and does that by making several assumptions. The benefit of applying such assumptions is that the insight in AM/PM conversion is increased as the simplified model greatly reduces the influences involved. The downside is, however, that the use of assumptions limits the applicability of the results and one should be critical: where do the results apply?

The simulations have been conducted in two separate steps. First, the ability of the simplified RC-circuit to resemble the behaviour of the HBT has been characterized. Second, the influence of the parameters in this RC-circuit on the AM/PM conversion effects have been identified and simulated. From the first step has been concluded that the RC-circuit is capable of modelling AM/PM conversion effects in the HBT when this device operates in a weakly nonlinear mode. However, the simulations conducted to verify this have been based on a select number of circuit configurations. It has not been checked with simulations if the impact of for instance the source resistance on the HBT on the one hand and on the RC-circuit on the other, are similar. The curves in Figure 41 already showed that the resistor impacts both circuits differently (although it is showing some similar behaviour: in both cases an increase in resistance value led to an increase in AM/PM conversion for low values and to a decrease for high values, but the point that defined the difference between ‘low’ and ‘high’ values was different). More research is needed to characterize the relation between the conclusions based on the RC-circuit and the behaviour of the HBT, though based on several simulations, like the one in Figure 41, one should already conclude that the applicability of the results is limited due to the fact that the analysis has been based on linear circuit analysis methods.

One should therefore use the presented simplified model as a tool in gaining more insight in the way that AM/PM conversion exhibits itself in transceiver systems and recognize that this comes at the cost of model accuracy. If the goal is to correctly model AM/PM conversion effects in HBTs, also for stronger nonlinearities, it would be better to resort to methods that are capable of accurately modelling nonlinear effects in dynamic nonlinear systems as discussed in Section 4.3.

Previous findings have been used in this research to model AM/PM conversion effects in transceiver systems. Maas et al. [4] have presented an equivalent circuit for the HBT. The nonlinearities (and their relative impact) these authors have presented in their model were a proper basis from which the simplified model has been derived. For the characterization of the AM/PM conversion in this simplified RC-circuit, the linearized approximation from Razavi [9] has proven to be a good starting point; especially qualitative conclusions from this thesis have verified previous research presented in his book RF Microelectronics [9].

However, discussion is required for several results that were not in line with the above-mentioned theory. The magnitude of most approximations did not match the simulations performed on the RC-circuit. Discrepancies were for several cases large (up to a difference of a factor 16) in which cases the approximation proved to be only good in a qualitative regard. In the results presented in this thesis, these differences between approximations and simulations have been accounted for by manually adding a compensation factor. Better would be to look into the origin of the differences such that they can be accounted for, but the limited time available required that this was postponed for future researchers.

Taking into account the discussion presented in this section, I would like to stress that one should see this thesis as a beginner's guide into AM/PM conversion in transceiver systems. Focus has been set to creating insight in the origin of AM/PM conversion effects in HBTs specifically and to characterizing these effects and the parameters that impact them. For accurate models of AM/PM conversion in transceiver systems one is advised to resort to research of others.

8.1 Recommendations for further research

The research conducted in this thesis can be further improved. Consider the recommendations for further research below:

- The applicability of the results obtained on the first-order low-pass RC-circuit with nonlinear capacitor regarding the reduction of AM/PM conversion effects on circuit containing HBTs should be looked into.
- The influence of the biasing point and/or biasing circuit on the capability of the RC-circuit to model the behaviour of the HBT should be assessed.
- The applicability of the results on the HBT should be extended to transceiver systems in general.
- An accurate model of AM/PM conversion in HBTs should be compiled and assessed using methods suited for the analysis of dynamic nonlinear systems.
- The resemblance between the deviation in zero-crossings for the HBT and the RC-circuit should be evaluated based on an FFT plot that shows the frequency components and their magnitudes, enabling much better comparison.

9 References

[1] N. Muhammad Amin and M. Weber, “Transmit and receive crosstalk cancellation,” 2010, pp. 210–215.

[2] S. Narayanan, “Transistor Distortion Analysis Using Volterra Series Representation,” *Bell Syst. Tech. J.*, vol. 46, no. 5, pp. 991–1024, May 1967.

[3] P. Wambacq, G. G. E. Gielen, P. R. Kinget, and W. Sansen, “High-frequency distortion analysis of analog integrated circuits,” *IEEE Trans. Circuits Syst. II Analog Digit. Signal Process.*, vol. 46, no. 3, pp. 335–345, Mar. 1999.

[4] S. A. Maas, B. L. Nelson, and D. L. Tait, “Intermodulation in heterojunction bipolar transistors,” *IEEE Trans. Microw. Theory Tech.*, vol. 40, no. 3, pp. 442–448, Mar. 1992.

[5] H. Jardón-Aguilar and J. Aguilar-Torrentera, “AM-PM conversion introduced by MESFET and HBT,” *Microw. Opt. Technol. Lett.*, vol. 33, no. 5, pp. 319–321, Jun. 2002.

[6] L. C. Nunes, P. M. Cabral, and J. C. Pedro, “A physical model of power amplifiers AM/AM and AM/PM distortions and their internal relationship,” 2013, pp. 1–4.

[7] S. Horst and J. D. Cressler, “AM/PM Nonlinearities in SiGe HBTs,” 2009, pp. 1–4.

[8] A. Borys and Z. Zakrzewski, “Use of Phasors in Nonlinear Analysis,” *Int. J. Electron. Telecommun.*, vol. 59, no. 3, Jan. 2013.

[9] B. Razavi, *RF microelectronics*, 2nd ed. Upper Saddle River, NJ: Prentice Hall, 2012.

[10] L. Spreeuwers, R. van Rootseler, and C. Zeinstra, “Circuit Analysis: Exercises, Summaries and Recipes.” University of Twente, Nov-2014.

[11] S. Golara, “Identifying Mechanisms of AM-PM Distortion.” University of California, 2015.

[12] F. Stein, D. Celi, C. Maneux, N. Derrier, and P. Chevalier, “Investigation of the base resistance contributions in SiGe HBT devices,” 2013, pp. 311–314.

10 Appendices

10.1 B&K-Analysis of 'Intermodulation in Heterojunction Bipolar Transistors' by Maas et al. [4]

1. *What is the object or phenomenon (X) for which the 'model for X' is produced in the paper?*

The paper discusses a model on the small-signal intermodulation distortion in heterojunction bipolar transistors. Since intermodulation distortion can only be present as a result of nonlinearities within a circuit, the paper discusses these nonlinearities in the context of heterojunction bipolar transistors. In HBTs, nonlinearities can mostly be found in the base-emitter capacitance, hence, this capacitance is characterized and an expression for the exact manifestation of nonlinearities is presented.

2. *What is the function or intended 'purpose' of the model constructed in the paper?*

The model will show what nonlinearities are present in HBTs through an equivalent circuit in which these nonlinearities have been included. This information can be used to characterize the effects of AM/AM conversion (intermodulation distortion) by performing simulations or calculations on this equivalent circuit.

Thus, the function of the model in the paper is to calculate and predict how AM/AM conversion effects manifest themselves in heterojunction bipolar transistors.

3. *What are the measurable quantities in the model?*

The model contains a few components, namely resistors and capacitors, of which the coefficients for the resistance or capacitance are measurable quantities. Next to that, as it concerns an electrical circuit, the current through and voltage across each component can be measured and calculated, so all of those are also measurable quantities. Then there is one more variable that is hidden in the exact expression for the capacitances and resistances described above, because both will depend on the temperature in which the circuit is operating.

The model can be used to predict AM/AM conversion, which is mostly characterized by the second- or third-order intercept point, but this is not an actual measurable quantity of the model itself and can only be indirectly simulated or calculated.

4. *What is the knowledge (theoretical/experimental) used in the construction of the model?*

The framework of the model has been based on the Volterra-series approximation. As it concerns a dynamic nonlinear system, finding an exact expression for the circuit transfer is not feasible, which is why it is common practice to approximate this transfer through the Volterra-series.

The authors use the nonlinear current source approach to apply the Volterra-series. This means that they will construct a circuit which will have linear circuit elements, but in which for each nonlinear element a current source has been placed in parallel with its linear equivalent. This current source will have the magnitude of the nonlinear component of the element expression. One can easily follow this approach in the paper by examining the figures. Figure 1 shows the linear equivalent I mentioned above and Figure 2 shows the inclusion of the nonlinear current components of the nonlinear circuit elements.

Results are subsequently acquired through mathematical reasoning. Known relations between charge, voltage and capacitance in capacitors are used as well as relations for the dependence on the emitter current on the base-emitter voltage. Knowledge on derivatives is also applied. Through the application

of this knowledge, the authors obtain expressions that can be used to calculate the second-order and third-order intercept points which I already briefly mentioned in question 3.

5. *What are the assumptions used in the construction of the model?*

The authors make several assumptions in the construction of the model:

- The source and load impedances of the transistor are assumed to be real.
- The dominant nonlinearities in the transistor are assumed to be the base-emitter junction capacitance and the nonlinear current gain, other nonlinearities will not be modelled.
- The transistor is assumed to be properly biased.
- The authors assume that the base-emitter capacitance is dominated by diffusion capacitance.
- It is assumed that $\boldsymbol{2R_b c_1 \omega_1 \gg 1}$.
- Finally, the relation between collector and emitter current is assumed to be linear and instantaneous and hence can be described by $\boldsymbol{I_C = \alpha I_e}$, while in reality a more accurate expression would be:

$$\boldsymbol{I_c = \alpha_1 I_e(t - t_d) + \alpha_2 I_e^2(t - t_d) + \alpha_3 I_e^3(t - t_d)}$$

6. *How is the model justified?*

The authors describe how the model has been simulated using C/NL (a program to evaluate Volterra-based models), from which calculations on the second-order (IP2) and third-order (IP3) intercept point have been extracted. These points have also been measured, and measured + calculated results have been plotted in Figure 4. An elaborate discussion on this plot can be found in the text. The authors explain which phenomena and/or assumptions give rise to the differences between the calculations and the measurements.

They state that a major factor in the differences is the difficulty of controlling the load and source impedance during the measurements. As calculations were done with a value of 50 Ω for both, any differences for these values in the measurements will cause defects in the results. Unfortunately, there is little discussion on what other effects might have influenced the difference between calculations and measurements, because I find it unlikely that the above described effect is the only factor.

Considering these experimental results in a much broader view, the above criticism probably follows from the fact that there is no explanation on *how* the measurement results were acquired. There is only a very brief statement on the transistor used, but not on other elements of the testing set-up. This makes it hard to reproduce the results and verify the research, which is important to consider when evaluating the justification of the model.

Next to that, the analysis that has been presented assumed real load and source impedances where they are generally complex. The authors trivialize this point by stating that the model shows that certain phenomena cancel each other anyway.

All in all, there *is* a justification of the model through measurements results, but the authors fail to provide the necessary information to be able to reproduce the results. In addition, one could say that the way the authors account for the differences between model and measurements testifies that the results have not been fully accounted for.

10.2 Derivation of the Approximation to the AM/PM Conversion Effects in Nonlinear RC-Networks

To be able to give an estimate or expression of the AM/PM conversion effects, one must first determine the circuit behaviour. This can be done by determining the differential equation of the system, calculating its solution and determining the phase of this solution.

Determining the differential equation

A differential equation will be determined for the circuit depicted in the Figure 10.2.1 below.

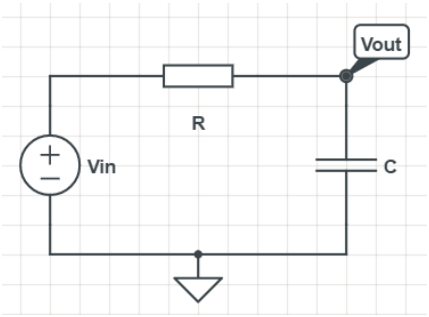

Figure 10.2.1: First-order low-pass RC-filter.

Recognizing that $Z_C = \frac{1}{j\omega C}$ and trough considering the circuit as an impedance divider one finds:

$$V_{out} = V_{in} \cdot \frac{1}{RCj\omega + 1}$$

Hence, considering a multiplication by $j\omega$ is equal to differentiation in the time domain:

$$RC \cdot \frac{dV_{out}(t)}{dt} + V_{out} = V_{in}$$

Solving the differential equation

The solution to the differential equation presented above consists of two parts: a homogeneous solution and a particular solution. The input has been taken to be $V_{in} = A\cos\omega t$. Both solutions can be found through solving the following two equations:

$$RC \cdot \frac{dV_{oh}(t)}{dt} + V_{oh}(t) = 0$$

$$RC \cdot \frac{dV_{op}(t)}{dt} + V_{op}(t) = A\cos\omega t$$

For $V_{oh}(t)$, $\alpha_2 e^{rt}$ can be substituted as a trial solution. Through differentiation and elimination, one ends up with:

$$RCr\alpha_2 e^{rt} + \alpha_2 e^{rt} = 0$$

Hence,

$$r = -\frac{1}{RC}$$

Thus, the homogeneous solution is in this case equal to:

$$V_{oh}(t) = \alpha_2 \cdot e^{-\frac{1}{RC}t}$$

The trial solution for the particular solution will be $\alpha_1 \cos(\omega t + \phi)$ and can also be substituted in the differential equation, one finds:

$$-\alpha_1 \omega \cos(\phi) \sin(\omega t) - \alpha_1 \omega \sin(\phi) \cos(\omega t) + \frac{1}{RC}[\alpha_1 \cos(\phi) \cos(\omega t) - \alpha_1 \sin(\phi) \sin(\omega t)] = \frac{A}{RC} \cos(\omega t)$$

Collecting respectively the terms $\cos(\omega t)$ and $\sin(\omega t)$, one finds:

$$-\alpha_1 \omega \sin(\phi) + \frac{1}{RC} \alpha_1 \cos(\phi) = \frac{A}{RC}$$

$$-\alpha_1 \omega \cos(\phi) - \frac{1}{RC} \alpha_1 \sin(\phi) = 0$$

Solving this for α_1 and ϕ yields:

$$\alpha_1 = \frac{A}{\cos(\phi) - \omega RC \sin(\phi)}$$

$$\phi = \arctan(-\omega RC)$$

Thus,

$$V_{op}(t) = \frac{A}{\cos(\phi) - \omega RC \sin(\phi)} \cos(\omega t + \arctan(-\omega RC))$$

AM/PM Conversion

When one looks at the AM/PM conversion effects only the steady state situation is of importance. Note that for $t \to \infty$ the homogeneous solution will equal zero. Considering that the capacitance will be described by the following nonlinear expression:

$$\mathrm{C} = \mathrm{C}_1 + \mathrm{C}_2 \cdot \mathrm{V}_\mathrm{C} + \mathrm{C}_3 \cdot \mathrm{V}_\mathrm{C}^2,$$

one can approximate the AM/PM conversion by writing the capacitance as $\mathrm{C(t)}$.

Assuming that the input frequency is below the cut-off frequency of the circuit ($\mathrm{RC(t)}\omega_1 \ll 1$ rad), and hence that the voltage across the capacitor is roughly equal to the input, one can rewrite the phase of the output voltage as:

$$\phi = -\mathrm{R}(\mathrm{C}_1 + \mathrm{C}_2 \cdot \mathrm{V}_\mathrm{o}(\mathrm{t}) + \mathrm{C}_3 \cdot \mathrm{V}_\mathrm{o}(\mathrm{t})^2)\omega = -\mathrm{R}(\mathrm{C}_1 + \mathrm{C}_2 \cdot \mathrm{A}\cos(\omega \mathrm{t}) + \mathrm{C}_3 \cdot \mathrm{A}^2 \cos(\omega \mathrm{t})^2)\omega$$

Denoting that $\cos(\omega \mathrm{t})^2$ can be rewritten as $\frac{1}{2} + \frac{1}{2}\cos(2\omega \mathrm{t})$, one can approximate the AM/PM conversion. Although the second-order capacitance constant also seems to yield phase modulation due to amplitude modulation at the input, even harmonics are suppressed in differential circuits and hence these effects do not manifest themselves in RF-circuits (as they are highly likely to be differential). The approximation can be written as follows:

$$\phi(\mathrm{A}) = -\frac{\mathrm{RC}_3 \omega \mathrm{A}^2}{2}$$

in which
- $\phi(A)$ is the amplitude dependent phase shift
- R is the value of the resistor in the RC-network in Ω
- C_3 is the third-order nonlinearity constant of the capacitance in F

- ω is the input frequency in $\frac{rad}{s}$
- A is the peak-amplitude of the input signal

10.3 Derivation of the Approximation to the AM/PM Conversion Effects in Extended Nonlinear RC-Networks

10.3.1 Derivation of AM/PM conversion effects in the extension of the first-order low-pass RC-filter with an extra resistor in parallel with the capacitor

To be able to give an estimate or expression of the AM/PM conversion effects, one must first determine the circuit behaviour. This can be done by determining the differential equation of the system, calculating its solution and determining the phase of this solution.

Determining the differential equation

A differential equation will be determined for the circuit depicted in Figure 10.3.1.1.

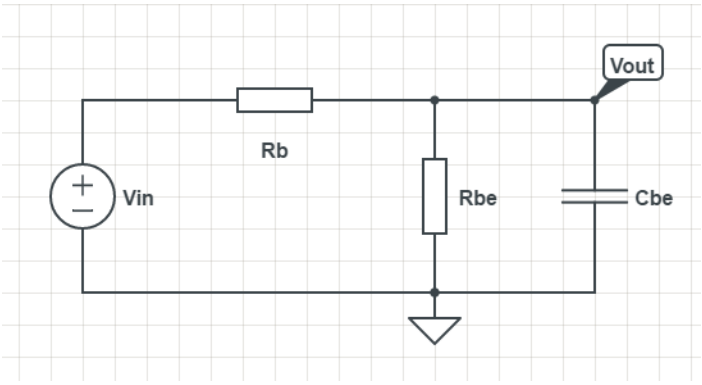

Figure 10.3.1.1: First-order low-pass RC-filter with additional resistor in parallel with the capacitor.

Recognizing that $Z_{C_{be}} = \frac{1}{j\omega C_{be}}$ and $Z_{R_{be}} = R_{be}$, one can make a single expression for the equivalent impedance of these elements:

$$R_{be}//C_{be} = \frac{\frac{R_{be}}{j\omega C_{be}}}{R_{be} + \frac{1}{j\omega C_{be}}} = \frac{R_{be}}{R_{be}C_{be}j\omega + 1}$$

Trough considering the circuit as an impedance divider one finds:

$$V_{out} = V_{in} \cdot \frac{R_{be}}{R_b R_{be} C_{be} j\omega + R_b + R_{be}} = V_{in} \cdot \frac{1}{1 + \frac{R_b}{R_{be}} + R_b C_{be} j\omega}$$

Hence, considering a multiplication by $j\omega$ is equal to differentiation in the time domain:

$$R_b C_{be} \cdot \frac{dV_{out}(t)}{dt} + \left(\frac{R_b}{R_{be}} + 1\right) V_{out} = V_{in}$$

Solving the differential equation

The solution to the differential equation presented above consists of two parts: a homogeneous solution and a particular solution. The input has been taken to be $V_{in} = A\cos\omega t$. Both solutions can be found through solving the following two equations:

$$R_b C_{be} \cdot \frac{dV_{oh}(t)}{dt} + \left(\frac{R_b}{R_{be}} + 1\right) V_{oh}(t) = 0$$

$$R_b C_{be} \cdot \frac{dV_{op}(t)}{dt} + \left(\frac{R_b}{R_{be}} + 1\right) V_{op}(t) = A \cos \omega t$$

For $V_{oh}(t)$, $\alpha_2 e^{rt}$ can be substituted as a trial solution. Through differentiation and elimination, one ends up with:

$$R_b C_{be} r \alpha_2 e^{rt} + \left(\frac{R_b}{R_{be}} + 1\right) \alpha_2 e^{rt} = 0$$

Hence,

$$r = -\left(\frac{R_b}{R_b R_{be} C_{be}} + \frac{1}{R_b C_{be}}\right) = -\frac{R_b + R_{be}}{R_b R_{be} C_{be}}$$

Thus, the homogeneous solution is in this case equal to:

$$V_{oh}(t) = \alpha_2 \cdot e^{-\frac{R_b + R_{be}}{R_b R_{be} C_{be}} t}$$

The trial solution for the particular solution will be $\alpha_1 \cos(\omega t + \phi)$ and can also be substituted in the differential equation, one finds:

$$-\alpha_1 \omega \cos(\phi) \sin(\omega t) - \alpha_1 \omega \sin(\phi) \cos(\omega t) + \frac{(R_b + R_{be})}{R_b R_{be} C_{be}} [\alpha_1 \cos(\phi) \cos(\omega t) - \alpha_1 \sin(\phi) \sin(\omega t)] = \frac{A}{R_b C_{be}} \cos(\omega t)$$

Collecting respectively the terms $\cos(\omega t)$ and $\sin(\omega t)$, one finds:

$$-\alpha_1 \omega \sin(\phi) + \frac{R_b + R_{be}}{R_b R_{be} C_{be}} \alpha_1 \cos(\phi) = \frac{A}{R_b C_{be}}$$

$$-\alpha_1 \omega \cos(\phi) - \frac{R_b + R_{be}}{R_b R_{be} C_{be}} \alpha_1 \sin(\phi) = 0$$

Solving this for α_1 and ϕ yields:

$$\alpha_1 = \frac{A}{\frac{R_b + R_{be}}{R_{be}} \cos(\phi) - \omega R_b C_{be} \sin(\phi)}$$

$$\phi = \arctan\left(-\frac{\omega R_b R_{be} C}{R_b + R_{be}}\right)$$

Thus,

$$V_{op}(t) = \frac{A}{\frac{R_b + R_{be}}{R_{be}} \cos(\phi) - \omega R_b C_{be} \sin(\phi)} \cos\left(\omega t + \arctan\left(-\frac{\omega R_b R_{be} C}{R_b + R_{be}}\right)\right)$$

AM/PM Conversion

When one looks at the AM/PM conversion effects only the steady state situation is of importance. Note that for $t \to \infty$ the homogeneous solution will equal zero. Considering that the capacitance will be described by the following nonlinear expression:

$$C_{be} = C_1 + C_2 \cdot V_C + C_3 \cdot V_C^2,$$

one can approximate the AM/PM conversion by writing the capacitance as $C(t)$.

Assuming that the input frequency is below the cut-off frequency of the circuit ($RC(t)\omega_1 \ll 1\ \mathrm{rad}$), and hence that the voltage across the capacitor is roughly equal to the input, one can rewrite the phase of the output voltage as:

$$\begin{aligned}\phi &= -\frac{R_b R_{be}}{R_b + R_{be}}(C_1 + C_2 \cdot V_o(t) + C_3 \cdot V_o(t)^2)\omega \\ &= -\frac{R_b R_{be}}{R_b + R_{be}}(C_1 + C_2 \cdot A\cos(\omega t) + C_3 \cdot A^2\cos(\omega t)^2)\omega\end{aligned}$$

Denoting that $\cos(\omega t)^2$ can be rewritten as $\frac{1}{2} + \frac{1}{2}\cos(2\omega t)$, one can approximate the AM/PM conversion with the following expression:

$$\phi(A) = -\frac{R_b R_{be} C_3 \omega A^2}{2(R_b + R_{be})}$$

in which
- $\phi(A)$ is the amplitude dependent phase shift
- R_b is the value of the resistor in the original RC-network in Ω
- R_{be} is value of the additional resistor in parallel with the capacitor in Ω
- C_3 is the third-order nonlinearity constant of the capacitance in F
- ω is the input frequency in $\frac{rad}{s}$
- A is the peak-amplitude of the input signal

Based on the approximation above, a hypothesis can be formulated. If R_b and C_3 remain fixed, increasing R_{be} to infinity should lead to a similar effect as in the simple RC-filter. Consider:

$$\lim_{R_{be}\to\infty} \phi(A) = -\frac{R_b C_3 \omega A^2}{2}$$

On the other hand, if R_{be} is decreased to zero, one would short the capacitor and its corresponding nonlinear behaviour; the phase conversion will be zero:

$$\lim_{R_{be}\to 0} \phi(A) = 0$$

Combining these limits, one would expect that an increase in R_{be} would lead to AM/PM conversion effects that transition from being zero to equalling the behaviour of a first-order low-pass RC-filter.

10.3.2 Derivation of AM/PM conversion effects in the extension of the first-order low-pass RC-filter with the source impedance

Consider the circuit in Figure 10.3.2.1.

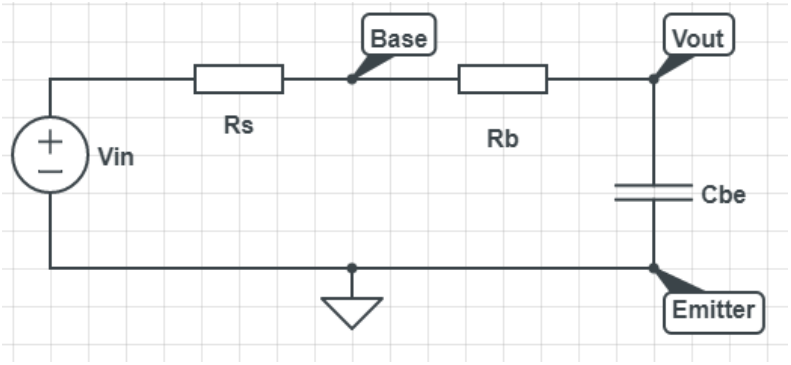

Figure 10.3.2.1: RRC-circuit resembling the simplified internal base-emitter structure of an HBT including the source resistance of the signal applied to the base.

The AM/PM conversion effects at the base can be approximated by applying linear phasor analysis and inserting the nonlinear capacitance expression in a later stage.

For the transfer function one finds:

$$V_o(t) = V_i(t) \cdot \frac{R_b + \frac{1}{j\omega C_{be}}}{R_s + R_b + \frac{1}{j\omega C_{be}}}$$

$$H(j\omega) = \frac{R_b C_{be} j\omega + 1}{(R_s + R_b) C_{be} j\omega + 1}$$

To determine the steady state response, transform back to the time-domain:

$$V_o(t) = Re\{Ye^{j\omega t}\} = |H(j\omega)| A \cos\big(\omega t + \phi + \arg\big(H(j\omega)\big)\big)$$

$$|H(j\omega)| = \frac{\sqrt{(R_b C_{be}\omega)^2 + 1}}{\sqrt{\big((R_s + R_b) C_{be}\omega\big)^2 + 1}}$$

$$\arg\big(H(j\omega)\big) = \arctan\left(\frac{\omega R_b C_{be}}{1}\right) - \arctan\left(\frac{(R_s + R_b) C_{be}\omega}{1}\right)$$

For the output, this yields:

$$V_o(t) = \frac{A\sqrt{(R_b C_{be}\omega)^2 + 1}}{\sqrt{\big((R_b + R_s) C_{be}\omega\big)^2 + 1}} \cos\big[\omega t + \arctan(\omega R_b C_{be}) - \arctan\big((R_s + R_b) C_{be}\omega\big)\big]$$

$$= \frac{A\sqrt{(R_b C_{be}\omega)^2 + 1}}{\sqrt{\big((R_b + R_s) C_{be}\omega\big)^2 + 1}} \cos\left(\omega t + \arctan\left[\frac{-R_s C_{be}\omega}{1 + R_b (R_s + R_b) C_{be}^2 \omega^2}\right]\right)$$

This appears to be correct, consider:

$$\lim_{R_b \to 0} \big(V_o(t)\big) = \frac{A}{\sqrt{R_s^2 C_{be}^2 \omega^2 + 1}} \cos(\omega t + \arctan(-R_s C_{be}\omega))$$

The above expression is the same as the one that has been derived for the first-order low-pass RC-filter.

Extracting the phase from the expression for the output voltage can be done in the same way as in Appendix 10.3.1, through substitution of C_{be} by the nonlinear expression. Deriving this expression is difficult due to the elaborate nature of the terms, so the results will be calculated with the use of computer programs like MATLAB and Mathematica.

10.4 Zero-Crossings and AM/PM Conversion

10.4.1 Derivation of the Approximation of the Relation Between Zero-Crossings and AM/PM Conversion Effects

Consider the following expression from Appendix 10.2:

$$V_o(t) = \frac{A}{\cos(\phi) - \omega RC\sin(\phi)}\cos(\omega t + \arctan(-\omega RC))$$

To find the zero-crossings, equate it to zero:

$$\begin{aligned}
&V_o(t) = \frac{A}{\cos(\phi) - \omega RC\sin(\phi)}\cos(\omega t + \arctan(-\omega RC)) = 0\\
&\cos[\omega t + \arctan(-\omega RC)] = 0\\
&\omega t + \arctan(-\omega RC) = \frac{\pi}{2} + \pi \cdot k\\
&\omega t = \left(\frac{\pi}{2} + \pi \cdot k\right) + \arctan(\omega RC)\\
&t = \frac{1}{\omega}\left(\frac{\pi}{2} + \pi \cdot k + \arctan(\omega RC)\right)
\end{aligned}$$

Now substitute $C(t) = C_1 + C_2V_C + C_3V_C^2$, $V_C = A_c\cos\omega t$ and $A_c = A_m(1 + m\cos\omega_m t)$:

$$\begin{aligned}
t = \frac{1}{\omega}\Big(&\frac{\pi}{2} + \pi \cdot k\\
&+ \arctan\Big(\omega R\left(C_1 + C_2A_m(1 + m\cos\omega_m t)\cos\omega t\right.\\
&\left.+ C_3\big(A_m(1 + m\cos\omega_m t)\big)^2\cos^2\omega t\right)\Big)\Big)
\end{aligned}$$

in which
- t_{ZC} is the value of the kth zero-crossing in seconds
- ω is the value of the carrier frequency in rad/s
- R is the value of the resistor in Ohm
- C_1, C_2, C_3 are the 1st, 2nd and 3rd-order capacitance constants in Farad
- m is the modulation factor
- A is the peak-amplitude of the carrier wave in Volts
- ω_m is the frequency of the modulator signal in rad/s.

10.4.2 Mathematica code

```
Rs = 50;
C1 = 123*10^(-15);
C2 = 0*10^ (-15);
C3 = 84*10^(-15);
ω = 2*π*10^10;          (* Carrier frequency *)
Am =  0.1;                    (* Carrier amplitude *)
ωm = ω/10;              (* Modulation frequency *)
m = 0.5;                      (* Modulation factor *)
tsim = 0.5*10^(-8);
```

$$\text{datalinear} = \{t\}/.\,(\text{NSolve}[\text{Cos}[\omega * t + \text{ArcTan}[-\omega * \text{Rs} * (\text{C1})]] == 0 \&\& 0 \le t \le \text{tsim}, t, \text{Reals}]);$$

```
data={t} /. (NSolve[Cos[ω*t+ArcTan[-
ω*Rs*(C1+C2*Am*(1+m*Cos[ωm*t])*Cos[ω*t]+C3*(Am*(1+m*Cos[ωm*t])*Cos[ω*t])*(Am*(1+m*Cos[ωm*t])
*Cos[ω*t]))]]==0&&0<= t<= tsim, t,Reals]);

xvalues = Range[Length[datalinear]];
datatoplot=TemporalData[{datalinear-data},{xvalues}];

ListPlot[datatoplot,Joined-> True,AxesLabel->{"# Zero-crossing","t [s]"}]
Export["out2.mat",{datalinear-data} ]
```

10.4.3 MATLAB code

Thanks to Inês for providing the code.

```
%% Reads a file from a table with 4 columns:
% |time| zerocrossings_Vin| time |zerocrossings_Vo|

close all;
clear; clc;

str_leg = {};
filename1 = 'ZeroCross HBT base 10';
filename2 = 'ZeroCross RC 10'; %includes parasitics in the supply lines, no
input matching

zerocrossing_table_ol = csvread(['/',filename1,'.csv'],1);
str_leg{length(str_leg)+1} = filename1;
zerocrossing_table_cl_10 = csvread(['/',filename2,'.csv'],1);
str_leg{length(str_leg)+1} = filename2;

str_leg = strrep(str_leg,'_',' ');

Y=zerocrossing_table_ol;
S_10=zerocrossing_table_cl_10;

% S and Y
row=1;
time_ol = Y(Y(:,row)>0, row);
time_cl_10 = S_10(S_10(:,row)>0, row);

row=2;
zc_vo_ol=Y(Y(:,row)>0, row);
row=4;
zc_vi_ol=Y(Y(:,row)>0, row);

row=2;
zc_vo_cl_10=S_10(S_10(:,row)>0, row);
row=4;
zc_vi_cl_10=S_10(S_10(:,row)>0, row);

% steadystate in samples
steadystate=1800; %number of samples to skip
time_ol=time_ol(steadystate+1:end);
time_cl_10=time_cl_10(steadystate+1:end);

zc_vi_ol=zc_vi_ol(steadystate+1:end);
zc_vo_ol=zc_vo_ol(steadystate+1:end);

zc_vi_cl_10=zc_vi_cl_10(steadystate+1:end);
```

```
zc_vo_cl_10=zc_vo_cl_10(steadystate+1:end);

%select min length of all vectors
all_len = [length(time_ol),length(time_cl_10),...
                length(zc_vi_ol),length(zc_vo_ol),...
                length(zc_vi_cl_10),length(zc_vo_cl_10)];
correctlen = min(all_len);

%select latest zero crossings
time_ol = time_ol(length(time_ol)-correctlen+1:end);
time_cl_10=time_cl_10(length(time_cl_10)-correctlen+1:end);

zc_vi_ol = zc_vi_ol(length(zc_vi_ol)-correctlen+1:end);
zc_vo_ol = zc_vo_ol(length(zc_vo_ol)-correctlen+1:end);

zc_vi_cl_10=zc_vi_cl_10(length(zc_vi_cl_10)-correctlen+1:end);
zc_vo_cl_10=zc_vo_cl_10(length(zc_vo_cl_10)-correctlen+1:end);

open_loop=zc_vi_ol-zc_vo_ol;
closed_loop_10=zc_vi_cl_10-zc_vo_cl_10;


figure
hold on
mathematica = importdata('out2.mat');
plot(mathematica-mean(mathematica),'k','LineWidth', 3)
plot(closed_loop_10-mean(closed_loop_10),'m','LineWidth',3)
plot(open_loop-mean(open_loop),'k','LineWidth', 3)
hold off
grid on
set(gca,'FontSize',14)
title('AMPM @ output RC-circuit')
legend('Simulated RC','Simulated HBT' )
xlabel('samples')
ylabel('time(s)')
```

10.5 Additional simulation results

10.5.1 On the decision to change the input amplitude sweep

Figure 10.5.1.1 shows the collector voltage of the testbench circuit and the corresponding input.

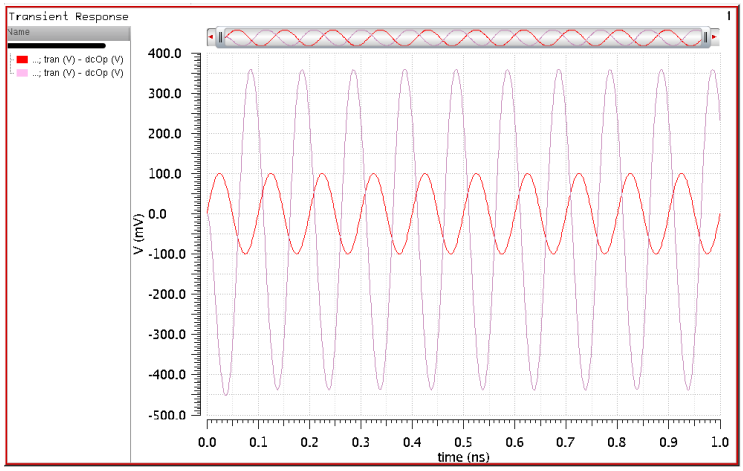

Figure 10.5.1.1: Transient simulation results of the input and collector voltage of the HBT inserted in the testbench circuit in Figure 14.

Visual inspection already shows that the transfer is not merely an amplification (V_{max} of the output is roughly 360 mV, while V_{min} is roughly -440 mV, as a result the average value of the output changes to a non-zero value). Figure 10.5.1.1 indicates that the applied amplitude is too large for a linear approximation of the variation around the bias point. The RC-network can only be verified as a good model for a weakly nonlinear phenomenon in the HBT if it is operating as weakly nonlinear. Therefore, the amplitude has been reduced to 50 mV_p to reduce the strength of the nonlinearities and the simulation in Figure 10.5.1.1 has been repeated, see Figure 10.5.1.2.

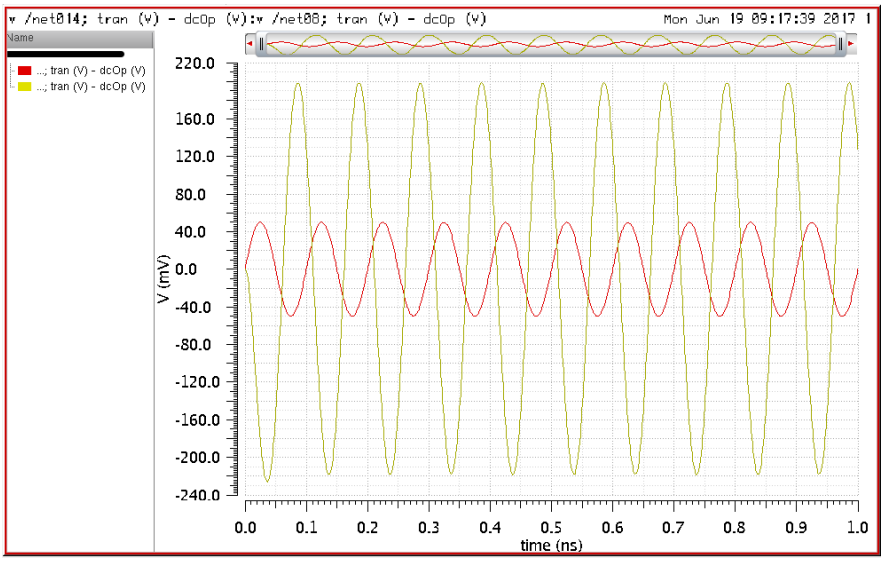

Figure 10.5.1.2: Transient simulation of the input applied to the HBT and the collector voltage of the circuit in Figure 14 for an input amplitude of 50 mV_p.

Figure 10.5.1.2 indeed seems to show that the signal at the collector has not been distorted by strong nonlinear behaviour and that a variation of 50 mV_p around the bias point of 900 mV can be approximated with linear behaviour; the average of the collector signal is still zero as opposed to the result in Figure 10.5.1.1.

10.5.2 On the decision to change the linear capacitance constant

The voltage across the capacitor of the RC-network should show similar behaviour as it is modelling the base of the HBT. Figure 10.5.1.3 shows these curves and the signal originating from the source.

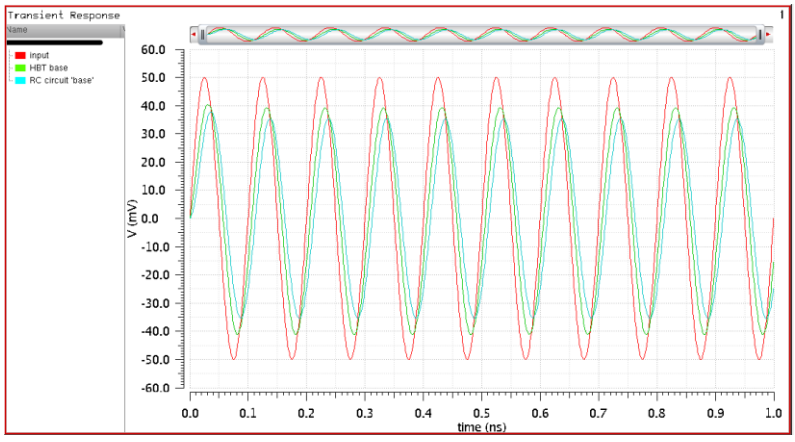

Figure 10.5.1.3: transient of figure 10.5.1.2 but now including the signal at the capacitor in the RC circuit.

Figure 10.5.1.3 is a clear indication that the linear phase shift of both circuits is different; the RC-curve is leading the curve of the signal at the base of the HBT. Apparently, the value of the linear capacitance

coefficient of the RC-network has been chosen too large. As a second attempt at approaching the correct value, the value as indicated by ProMOST will be used: 123 fF. Note that one has to be careful with basing parameters on data that will also be used to verify these same parameters, however, I deem it sufficiently justified due to the fact that these are fixed device parameters that can either be measured or chosen in the manufacturing of the device. Figure 10.5.1.4 shows the phase shift for the new value of $C_1 = 123\ fF$.

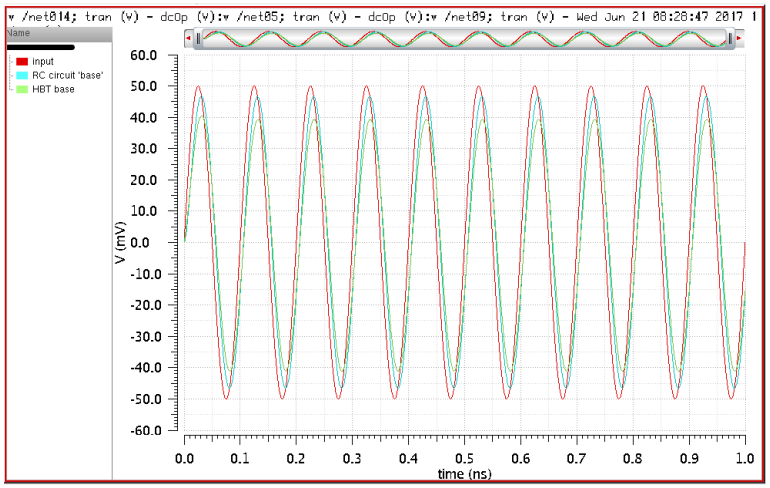

Figure 10.5.1.4: Transient of Figure 10.5.1.3 with the capacitance value indicated by ProMOST.

Considering that the nonlinear contributions to the phase are small compared to the linear component, Figure 10.5.1.4 now indeed shows that the signals at the 'base' of both the HBT and the RC-network overlap close to the zero-crossings indicating that the linear capacitance has now been properly estimated.

10.5.3 Showing various amplitude values in the verification of time domain zero-crossing modelling in the RC-circuit

The Figures 10.5.3.1 up to and including 10.5.3.4 below show the deviation in zero-crossing timing for both the simulated RC-circuit as the HBT circuit.

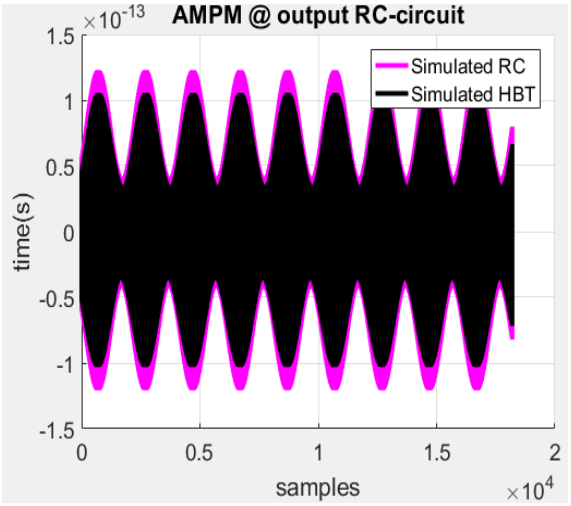

Figure 10.5.3.1: Deviation in zero-crossing timings simulated for both the HBT and RC-circuit. Input amplitude is equal to 10 mV_p.

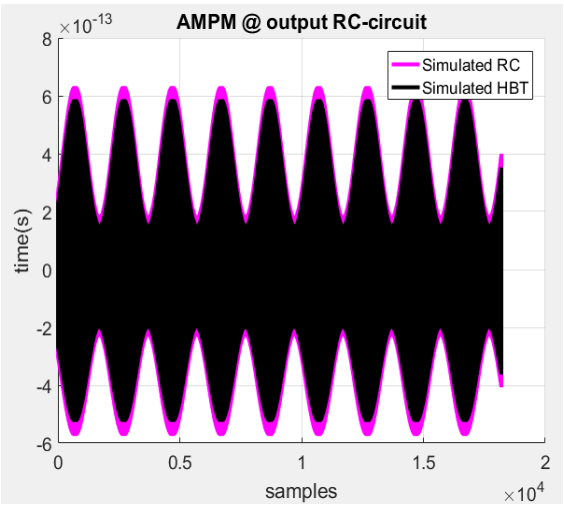

Figure 10.5.3.2: Deviation in zero-crossing timings simulated for both the HBT and RC-circuit. Input amplitude is equal to 50 mV_p.

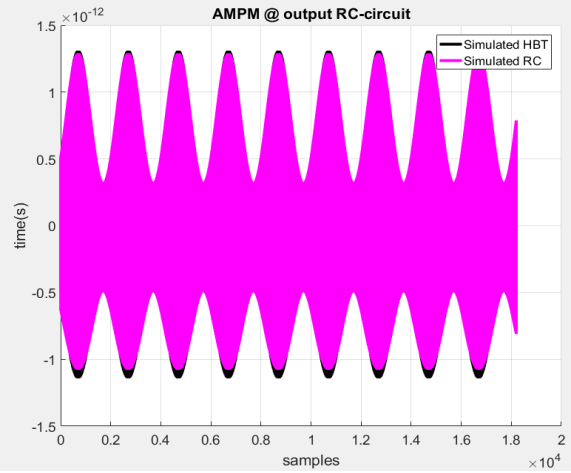

Figure 10.5.3.3: Deviation in zero-crossing timings simulated for both the HBT and RC-circuit. Input amplitude is equal to 100 mV_p.

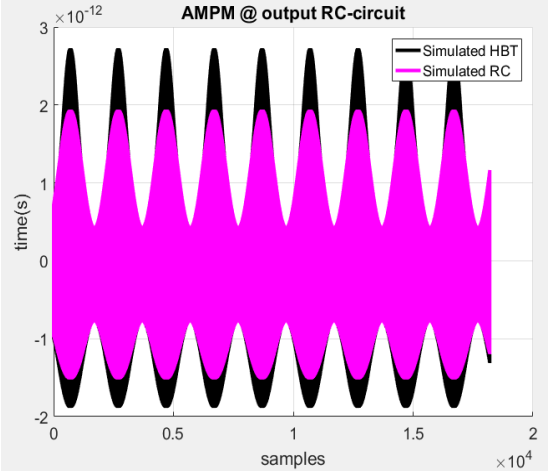

Figure 10.5.3.4: Deviation in zero-crossing timings simulated for both the HBT and RC-circuit. Input amplitude is equal to 150 mV_p.

10.6 Impact of the second-order capacitance constant on the AM/PM conversion effects in a first-order low-pass RC-filter

Figure 10.6.1 shows a sweep of the ratio between C_2 and C_1. Figure 10.6.2 shows a sweep in ratio between C_3 and C_1 and the influence various values of C_2 has on this relation.

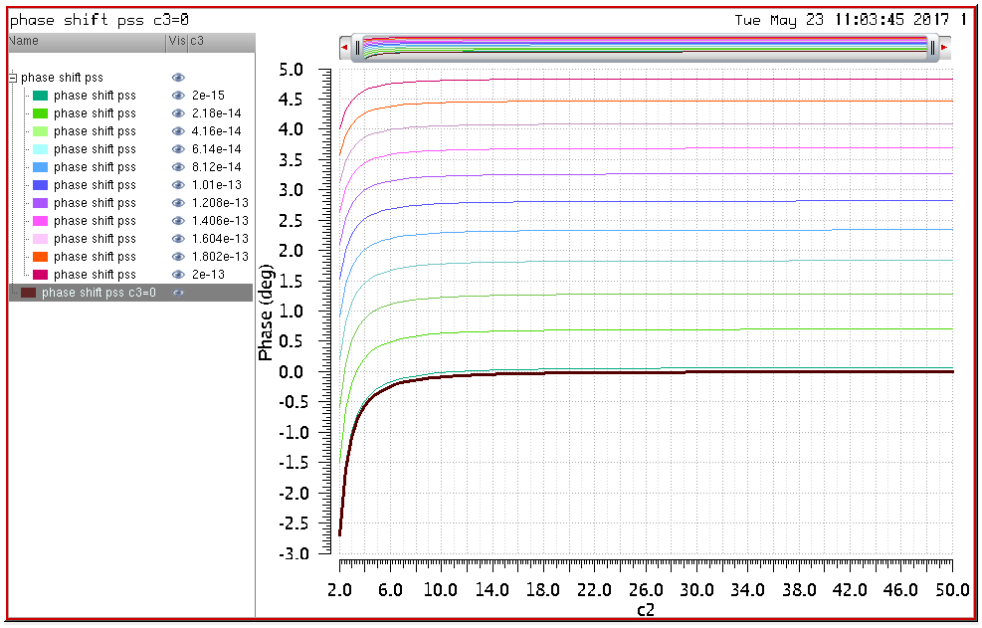

Figure 10.6.1: Sweep in ratio between C_1 and C_2. The x-axis represents the values of the ratio x in the equation $C_2 = C_1/x$. The value of C_3 for each curve can be found in the legend.

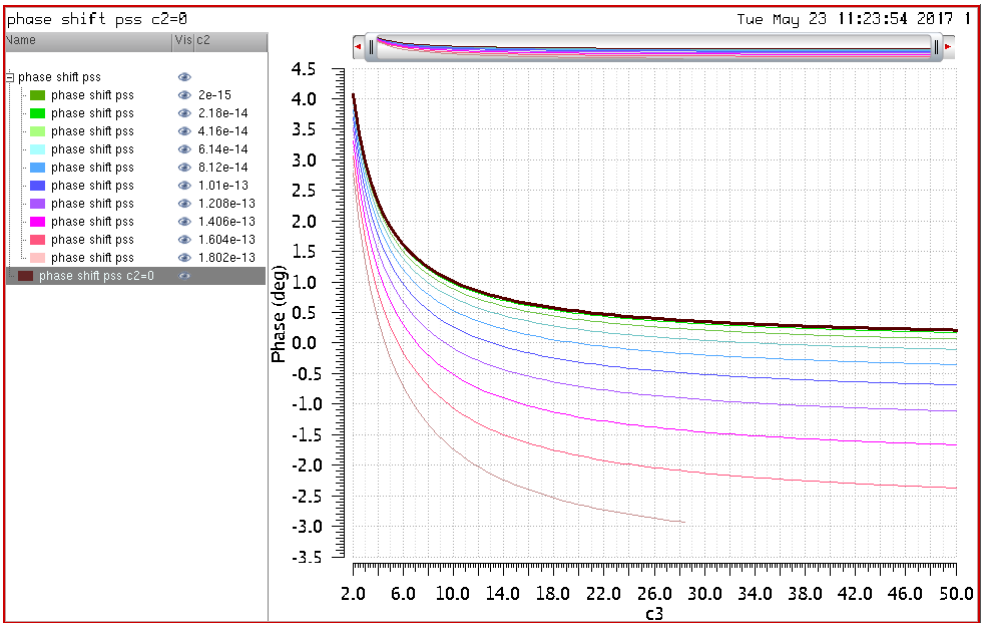

Figure 10.6.2: Sweep in ratio between C_1 and C_3. The x-axis represents the values of the ratio x in the equation $C_3 = C_1/x$. The value of C_2 for each curve can be found in the legend.

One can deduct from Figure 10.6.1 that only a relatively large value of C_2 with respect to C_1 has an influence on the AM/PM conversion effects. If C_2 is roughly 6 times smaller than C_1, its impact on the magnitude of the effects can already be neglected. Figure 10.6.1 shows a clear dependence on the value of the AM/PM conversion for an input amplitude value of 1 Volt on the value of C_3, which is in line with the results obtained on C_3.

Figure 10.6.2 shows that values of C_2 that are relatively large compared to C_1 will have a considerable influence on the impact of C_3 on the AM/PM conversion effects. Why do Figures 10.6.1 and 10.6.2 indicate that C_2 will have an influence (when it is relatively large), when the approximation states that this should not be the case? A plausible explanation is the fact that the simulations were performed on a single circuit, not a differential one. Even harmonics will be suppressed in a differential circuit.

To verify the above claim, the influence of C_2 has also been simulated in a differential circuit, see Figure 15 in Section 5.3. The default values for the circuit however still yielded amplitude modulated phase modulation, see Figure 10.6.3a. Figure 10.6.3b shows the magnitude of the AM/PM conversion for this case.

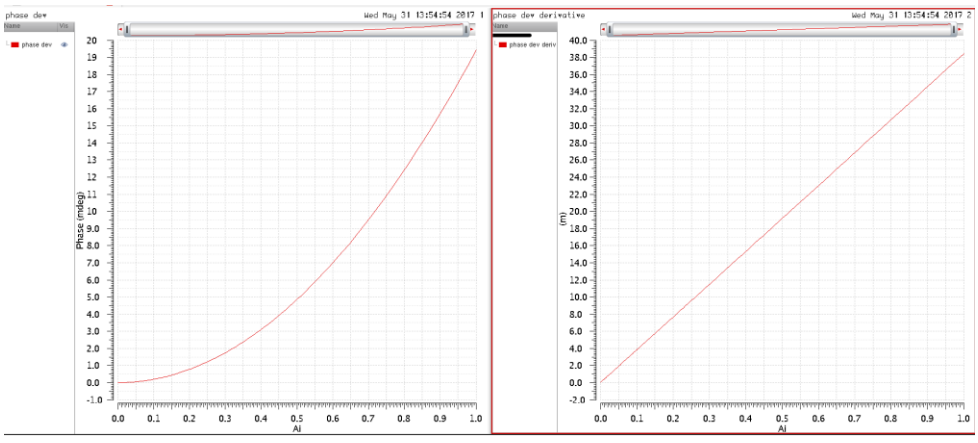

Figure 10.6.3 (a) and (b): 4a shows the phase shift for an amplitude sweep when C_3 has been set to zero and the other parameters to their default values. (b) shows the derivative of (a), showing the actual AM/PM conversion magnitude.

Why is there still AM/PM conversion present? The answer can be found in the simulation solver. It turns out that there are inaccuracies present in the zero-crossings of the time-domain simulations, yielding variations in phase shift. Plotting various amplitude values in the time-domain does not immediately show any discrepancies, see Figure 10.6.4. However, when one zooms in on the zero-crossings there is a clear shift in DC level and timing instant at which corresponding curves cross, see Figure 10.6.5.

Figure 10.6.5 clearly shows that the DC values of corresponding curves is shifting and that also the zero crossings are no longer located at one single timing instant. This will result in a phase shift that is related to the amplitude of the input signal and hence *appear* as AM to PM conversion.

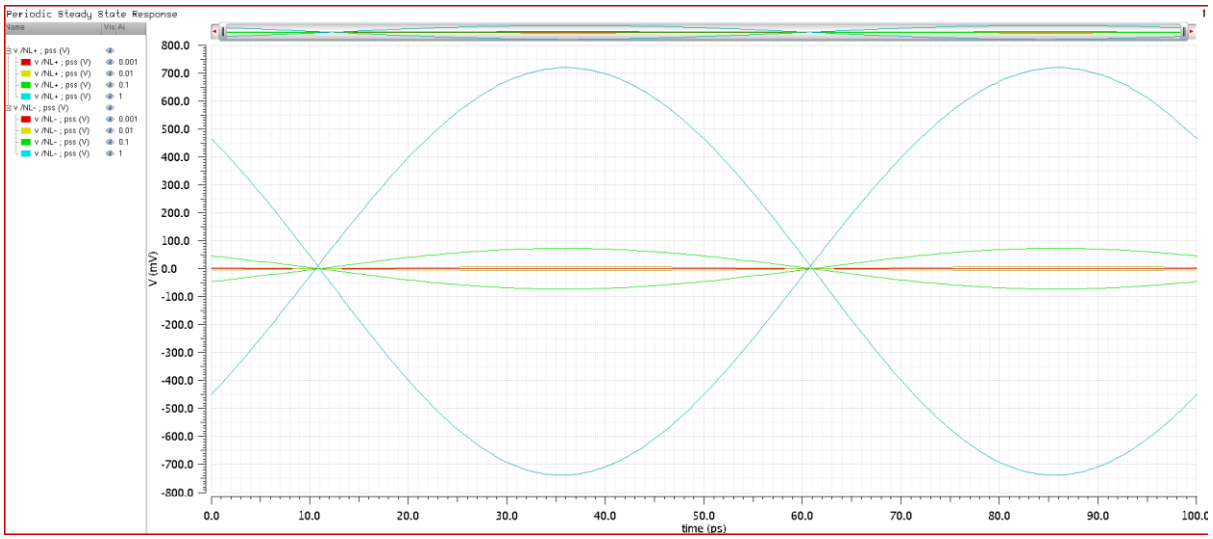

Figure 10.6.4: Time-domain voltage waveforms of the nonlinear outputs of the differential circuit with the settings of Figure 10.6.3.

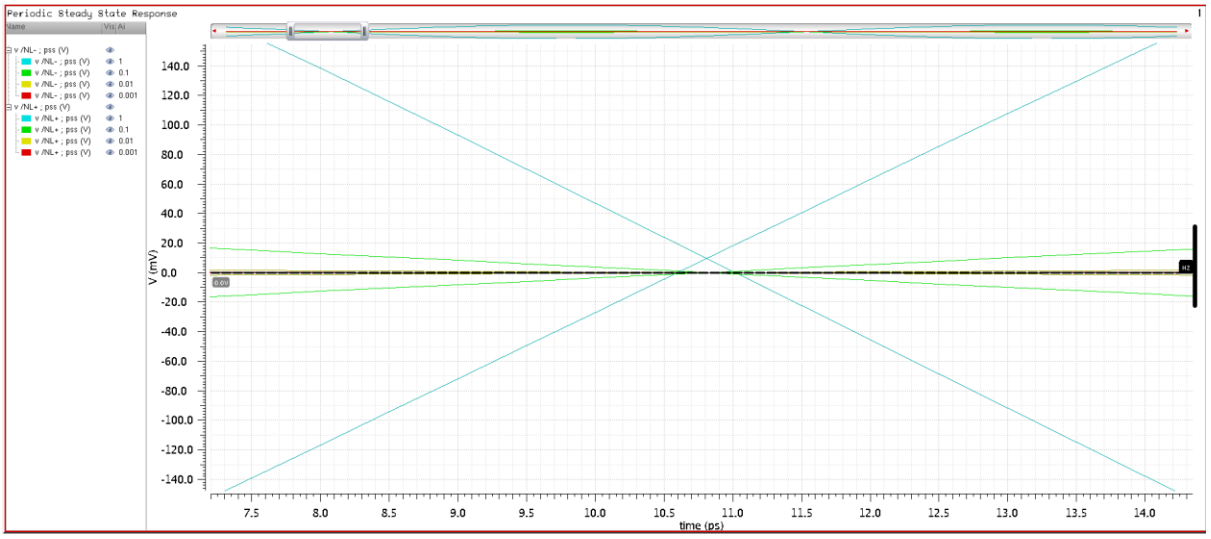

Figure 10.6.5: Plot of Figure 10.6.4 zoomed in upon a zero-crossing.

The effect shown in Figure 10.6.5 becomes more apparent in Figure 10.6.6 where more amplitude values have been plotted. If there would have not been any errors in phase, Figure 10.6.6 would have shown a single time on the x-axis at which all waves would have crossed.

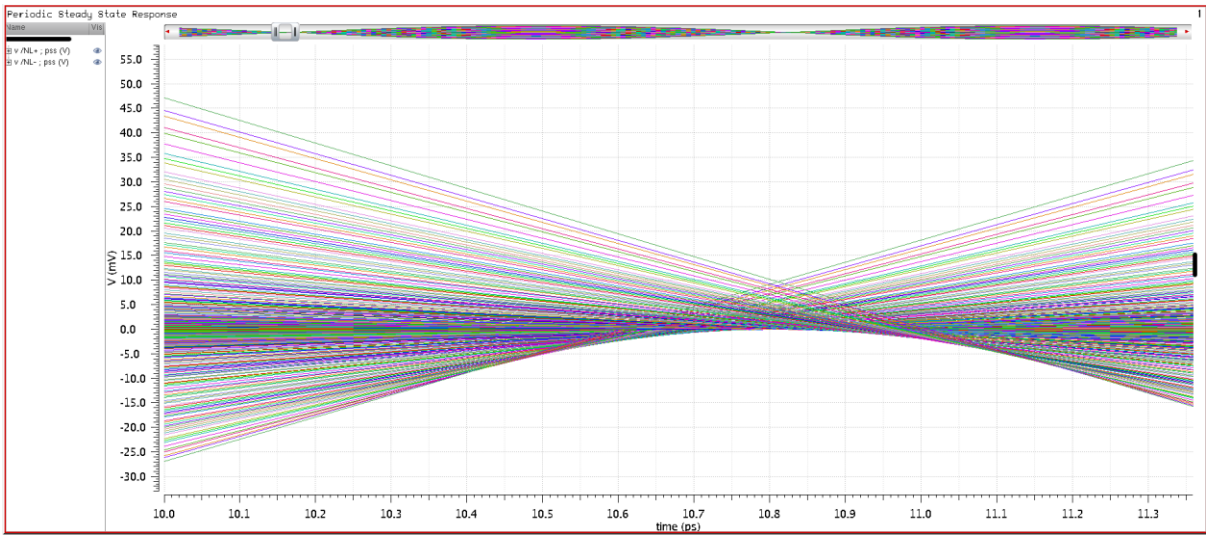

Figure 10.6.6: Time-domain voltage waveforms of the nonlinear outputs of the differential circuit with the settings of Figure 10.6.3 zoomed in upon a zero-crossing.

One could look into ways to prevent these effects. A possible solution could be decreasing the error tolerance of the simulations. However, the effects are small and one could wonder if it would be worth the extra processing power and time consumption to suppress the effects.